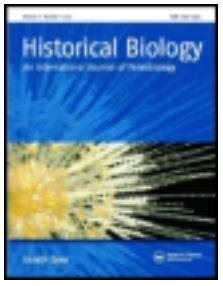

Historical Biology: An International Journal of Paleobiology

Publication details, including instructions for authors and subscription information:
http://www.tandfonline.com/loi/ghbi20

Redescription of Bonatitan reigi (Sauropoda: Titanosauria), from the Campanian-Maastrichtian of the Río Negro Province (Argentina)

L. Salgado[a], P.A. Gallina[bc] & A. Paulina Carabajal[d]

[a] Conicet - Instituto de Investigación en Paleobiología y Geología, Universidad Nacional de Río Negro, Isidro Lobo 516, 8332 General Roca, Río Negro, Argentina

[b] Conicet - Área de Paleontología, Fundación Félix de Azara, Argentina

[c] CEBBAD - Universidad Maimónides, Hidalgo 775, 7°piso, Buenos Aires, Argentina

[d] Conicet - Museo "Carmen Funes", 8318 Plaza Huincul, Neuquén, Argentina

Published online: 16 Apr 2014.

To cite this article: L. Salgado, P.A. Gallina & A. Paulina Carabajal (2014): Redescription of Bonatitan reigi (Sauropoda: Titanosauria), from the Campanian-Maastrichtian of the Río Negro Province (Argentina), Historical Biology: An International Journal of Paleobiology, DOI: 10.1080/08912963.2014.894038

To link to this article: http://dx.doi.org/10.1080/08912963.2014.894038

Historical Biology, 2014
http://dx.doi.org/10.1080/08912963.2014.894038

Taylor & Francis
Taylor & Francis Group

Redescription of *Bonatitan reigi* (Sauropoda: Titanosauria), from the Campanian–Maastrichtian of the Río Negro Province (Argentina)

L. Salgado[a]*, P.A. Gallina[b,c1] and A. Paulina Carabajal[d2]

[a]*Conicet – Instituto de Investigación en Paleobiología y Geología, Universidad Nacional de Río Negro, Isidro Lobo 516, 8332 General Roca, Río Negro, Argentina;* [b]*Conicet – Área de Paleontología, Fundación Félix de Azara, Argentina;* [c]*CEBBAD – Universidad Maimónides, Hidalgo 775, 7°piso, Buenos Aires, Argentina;* [d]*Conicet – Museo "Carmen Funes", 8318 Plaza Huincul, Neuquén, Argentina*

(*Received 19 October 2013; accepted 10 February 2014*)

The titanosaur sauropod *Bonatitan reigi* is redescribed. The material collected, originally interpreted as pertaining to two different individuals, is reorganised in five individuals, and the original type specimen is separated into three different individuals. One of the braincases is designated as a new type specimen. Some materials are described by the first time (sacral ribs, distal caudal, chevrons, metacarpals, astragalus and metatarsals), others reinterpreted as different bones ('ulna' and 'radius'). The diagnosis of *B. reigi* is emended, removing some of the original characters (longitudinal groove located on the suture between the parietals that continues posteriorly over the supraoccipital to the foramen magnum) and adding some new (small paired pits on the frontals and posterior ridge of the metacarpal IV). The phylogenetic analysis does not support *B. reigi* as a member of the Saltasaurinae, but rather as a basal member of a broad clade of sauropods that in turn is recovered as the sister group of the Saltasauridae.

Keywords: Sauropoda; Titanosauria; Bonatitan; Upper Cretaceous; Patagonia

1. Introduction

The titanosaur sauropod *Bonatitan reigi* was erected by Martinelli and Forasiepi (2004) on the basis of a series of disarticulated bones collected by J.F. Bonaparte between 1990 and 1994 in the surroundings of Salitral de Santa Rosa, Río Negro Province (Argentina). These authors stated that the material represents two different individuals, based on their relative sizes (Martinelli and Forasiepi 2004, p. 274). One of these (MACN-PV RN 821) was designated holotype; the other one (MACN-PV RN 1061) as 'referred material'. Also, Martinelli and Forasiepi (2004) assumed that these two individuals were of different size, being the MACN-PV RN 821 the larger (and the older). Finally, they placed *Bonatitan* among the Saltasaurinae within Titanosauria, although without the support of a phylogenetic analysis, only based on the presence of three characters, supposedly diagnostic of this subfamily of sauropods: (1) anterodorsal edge of the neural spine at the posterior level of the postzygapophyses in the middle caudal neural arch (taken from Salgado et al. 1997), (2) distal femoral condyles anteriorly exposed (taken from Wilson 2002) and (3) cancellous osseous tissue in the presacral and caudal vertebrae, mainly observed in the neural arches (modified from Powell 1986 and Wilson 2002). In fact, these characters were proposed as synapomorphies of Saltasaurinae by the cited authors; however, the phylogenetic definition of that clade is different in Salgado et al. (1997) and Wilson (2002), as Martinelli and Forasiepi (2004) acknowledge.

In this paper, we provide a full redescription of the material assigned to *B. reigi*, re-evaluate the number of individuals present in the quarry, describe material not included in the original description, provide a new diagnosis for the genus and species, and performed a phylogenetic analysis in order to test the hypothesis that *Bonatitan* is a Saltasaurine, which, by the way, was corroborated in the only analysis where *Bonatitan* was included (Filippi et al. 2011).

Institutional abbreviations: FGGUB, Faculty of Geology and Geophysics of the University of Bucharest, Romania; MACN-Pv RN, Museo Argentino de Ciencias Naturales 'Bernardino Rivadavia', colección de paleontología de vertebrados, Río Negro; MAU-PV-AG, Museo 'Argentino Urquiza', colección de paleontología de vertebrados; MGPIFD-GR, Museo de Geología y Paleontología del Instituto de Formación Docente Continua de General Roca, Río Negro, Argentina; MML, Museo Paleontológico de Lamarque, Río Negro, Argentina; MPCA, Museo Provincial 'Carlos Ameghino', Cipolletti, Río Negro, Argentina; MUCPv, Museo de Geología y Paleontología de la Universidad Nacional del Comahue, Neuquén, Argentina.

*Corresponding author. Email: lsalgado@unrn.edu.ar

2. Results

2.1 *Systematic palaeontology*

Dinosauria Owen, 1842

Sauropoda Marsh, 1878

Titanosauriformes Salgado, Coria and Calvo, 1997

Somphospondyli Wilson and Sereno, 1998

Titanosauria Bonaparte and Coria, 1993

Bonatitan Martinelli and Forasiepi, 2004

Bonatitan reigi Martinelli and Forasiepi, 2004

2.2 *Minimum number of individuals of* B. reigi

Martinelli and Forasiepi (2004) stated that the two specimens identified by them (MACN-PV RN 821 and MACN-PV RN 1061) were disarticulated and collected in the same quarry. According to Salgado et al. (2007), the level that yielded the materials of *B. reigi* corresponds to the lower of two subunits in which the Allen Formation (Campanian–Maastrichtian) is divided in the area of Salitral de Santa Rosa–Salinas de Trapalcó. It consists of thin sandy deposits with subordinated muddy levels, and thin evaporitic layers. According to these authors, all the lower subunit would correspond to a brackish lagoonal and supratidal environment, associated to aeolian sandy deposits and ephemeral rivers. Precisely, all *Bonatitan* remains were found in a sandy level, from which, not so far (50 m to the north approximately), the type specimen of the dromaeosaur theropod *Austroraptor cabazai* was collected (Novas et al. 2008); such level corresponds, in other sectors of the same area, to the 'egg level 1' of Salgado et al. (2007).

After a re-evaluation of the material catalogued as *B. reigi*, we distinguished five individuals. Most of this material was included in the original description of Martinelli and Forasiepi (2004). Our re-organisation of the material is based on the size and relative proportions of the different bones, and on the comparison with other, more complete titanosaurs, such as *Rapetosaurus* (Curry Rogers and Forster 2004; Curry Rogers 2009) and *Bonitasaura* (MPCA 460/467). To avoid confusions, we will maintain the original numeration of the specimens. The individuals recognised in this contribution are the following:

2.2.1 *Individual A*

(1) A complete anterior caudal vertebra. (2) The incomplete right tibia originally published as MACN-PV RN 821. (3) The metacarpal IV (described as ulna by Martinelli and Forasiepi 2004). (4) The undescribed metacarpal I MACN-PV RN 821. (5) The metatarsal I published as MACN-PV RN 1061 (Martinelli and Forasiepi 2004, Fig. 18G). (6) A proximal fragment of a metatarsal III. (7) A proximal fragment of a metatarsal V, not described (Figures 1 and 2).

2.2.2 *Individual B*

(1) The braincase referred to the specimen MACN-PV RN 1061 by Martinelli and Forasiepi (2004) (Figures 3 and 4). This braincase is slightly larger than the one originally assigned to specimen MACN-PV RN 821, although it seems to correspond to an earlier ontogenetic stage (because the sutures are not obscured by fusion). (2) The centrum of a cervical vertebra, originally published as belonging to the specimen MACN-PV RN 1061 (Martinelli and Forasiepi 2004, Fig. 9) (Figure 5(a)–(d)). (3) The centrum of a dorsal vertebra, originally considered as MACN-PV RN 821 (Martinelli and Forasiepi 2004, Figs 10 and 11) (Figure 5(e)–(h)). (4) A neural arch of a mid dorsal vertebra, possibly more anterior than the element 3, originally published as part of specimen MACN-PV RN 821 (Martinelli and Forasiepi 2004, Figs 10 and 11) (Figure 5(i)–(m)) (Figure 6–10). (5) A sacral rib catalogued as MACN-PV RN 821, not described (Figure 7(a),(b)). (6) A neural arch of a mid caudal vertebra, originally considered as part of specimen MACN-PV RN 821 (Martinelli and Forasiepi 2004, Fig. 16) (Figure 6(e)–(h)). (7) The appendicular bones of this individual include the left tibia originally published as MACN-PV RN 821 (Figure 11(b)), which practically articulates with the fibula MACN-PV RN 821 (Figure 12 (a)), and an undescribed astragalus mentioned as the calcaneous of the specimen MACN-PV RN 821 (Figure 12 (b)). All this material is slightly smaller than that of the individual A. (8) Both femora figured as MACN-PV RN 821 (Figure 10(a),(b)).

2.2.3 *Individual C*

A braincase published as part of the specimen MACN-PV RN 821 (Figures 1 and 2); it is the better preserved of both braincases. It could correspond to an individual even smaller than the individual B but larger than the individual D. This assumption is based on comparison with *Rapetosaurus*, a well-known titanosaur with cranial and postcranial remains.

2.2.4 *Individual D*

Most of the material originally included in specimen MACN-PV RN 1061 would correspond to this individual; the individual D is 20% smaller than the individual B (based on the comparison of the femora). The individual D is represented by a series of bones, which are mostly appendicular: (1) a humerus, assigned to specimen MACN-PV RN 821 by Martinelli and Forasiepi (2004) (Figure 8). (2) A femur published as MACN-PV RN 1061 by Martinelli and Forasiepi (2004) (Figure 10(c)). (3) A left tibia published as MACN-PV RN 1061 by Martinelli and Forasiepi (2004) (Figure 11(c)). (4) An astragalus

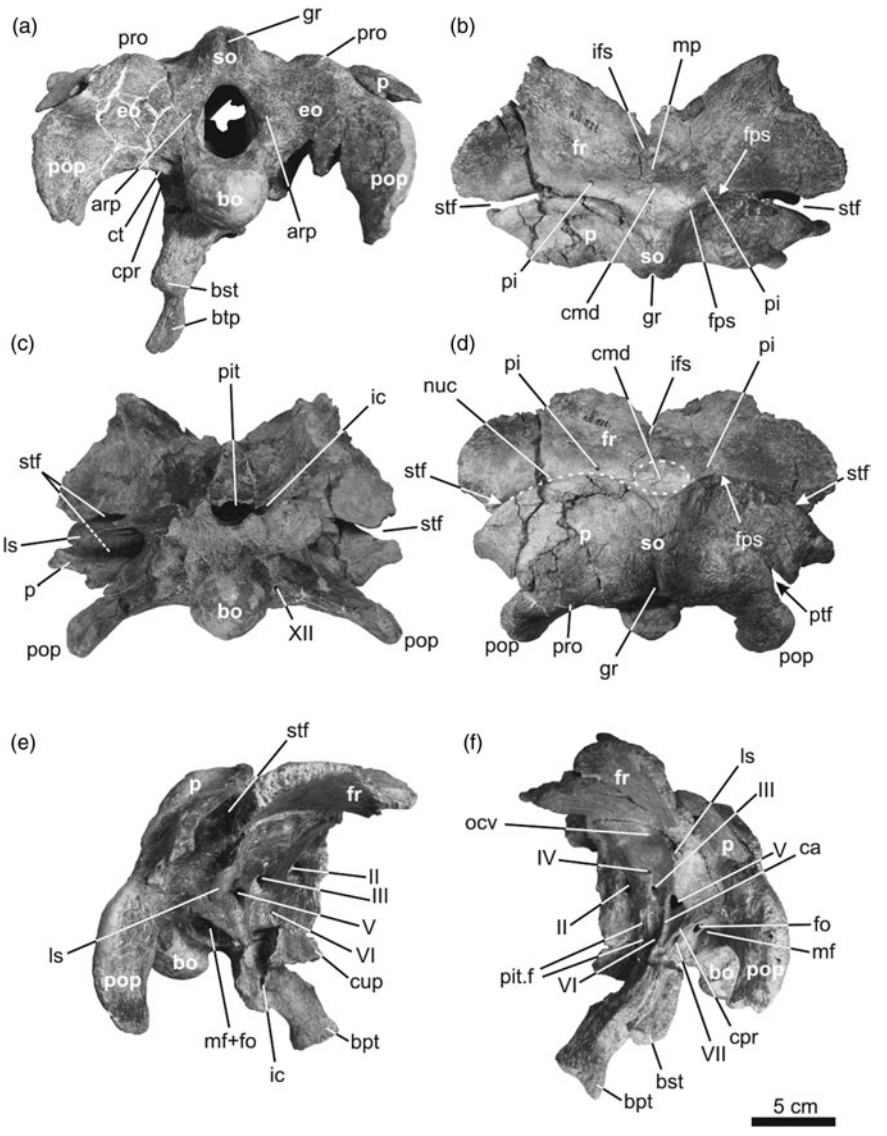

Figure 1. *B. reigi*. Holotype (MACN-PV RN 821). Braincase in posterior (a), dorsal (b), ventral (c), posterodorsal (d), right lateral (e) and left lateral (f) views. Abbreviations: arp, articulation for the proatlas; bo, basioccipital; bst, basisphenoid tubera; btp, basipterygoid process; ca, crista antotica; cmd, circular median depression; cpr, crista prootica; ct, crista tuberalis; cup, cultriform process; eo, exoccipital; fo, fenestra ovalis; fps, fronto-parietal suture; fr, frontal; gr, groove; ic, internal carotid; ifs, interfrontal suture; ls, laterosphenoid; mf, metotic foramen; mp, median protuberance; nuc, nuchal crest; ocv, orbitocerebral vein; p, parietal; pi, pit; pit, pituitary fossa; pit.f, pituitary foramina; pop, paroccipital process; pro, prominence; ptf, postemporal fenestra; so, supraoccipital; stf, supratemporal fenestra.

published as MACN-PV RN 1061 by Martinelli and Forasiepi (2004) (Figure 12(c)). (5) Many metatarsals, all without numeration; two fragments of a metatarsal V, not described (Figure 13(f),(g)); a distal fragment of a metatarsal III, not described (Figure 13(e)); and a proximal fragment of a metatarsal I, not described (Figure 13(d)), and one ungueal phalanx (Figure 13(i)). In addition, one complete metatarsal III (Figure 13(h)) is preliminarily assigned to this individual. (6) Many innumerate haemal arches, at least six, which are very small to belong to the larger individual B, and probably correspond to the individual D (Figure 7(c)).

2.2.5 *Individual E*

This individual is represented by a metacarpal V and a metacarpal I (described as MACN-PV RN 1061) (Figure 9 (c),(d)). It is the smallest individual, being 35% smaller than the individual A. A distal caudal vertebra without numeration and not described (Figure 6(i),(j)) also pertains to this individual.

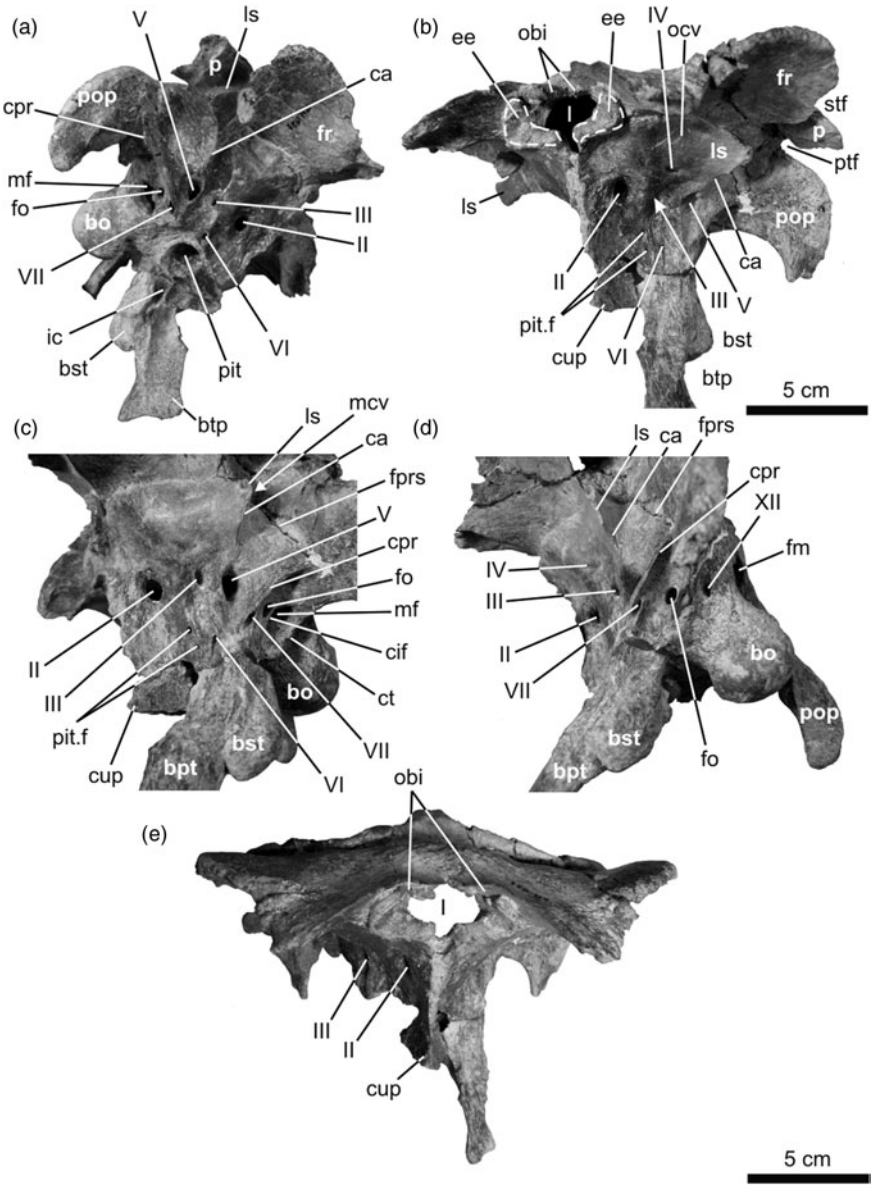

Figure 2. *B. reigi*. Holotype (MACN-PV RN 821). Braincase in right ventrolateral (a), left anterolateral (b), left lateral (detail of the orbital region) (c), left posterolateral (d) and anterodorsal (e) views. Abbreviations: bo, basioccipital; bst, basisphenoid tubera; btp, basipterygoid process; ca, crista antotica; cif, crista interfenestralis; cpr, crista prootica; ct, crista tuberalis; cup, cultrifrom process; ee, ethmoidal elements; fm, foramen magnum; fo, fenestra ovalis; fprs, fronto-prootic suture; fr, frontal; ic, internal carotid; ls, laterosphenoid; mcv, middle cerebral vein; mf, metotic foramen; obi, olfactory bulbes impressions; ocv, orbitocerebral vein; p, parietal; pit, pituitary fossa; pit.f, pituitary foramina; pop, paroccipital process; ptf, postemporal fenestra; stf, supratemporal fenestra.

2.3 Nomenclatorial acts

According to our interpretation, the components of the original holotype are actually distributed to three different individuals of different sizes: A, B and C. For this reason, we propose the exclusion of several components of the holotype following the art. 73.1.5 of the International Code of Zoological Nomenclature: 'If a subsequent author finds that a holotype which consists of a set of components (e.g. disarticulated body parts) is not derived from an individual animal, the extraneous components may, by appropriate citation, be excluded from the holotype.' In this way, we select the braincase of the individual C as the Holotype specimen, excluding all the other elements labelled with number MACN-PV RN 821. This choice is based on the systematic relevance of this element, as well as for its good preservation.

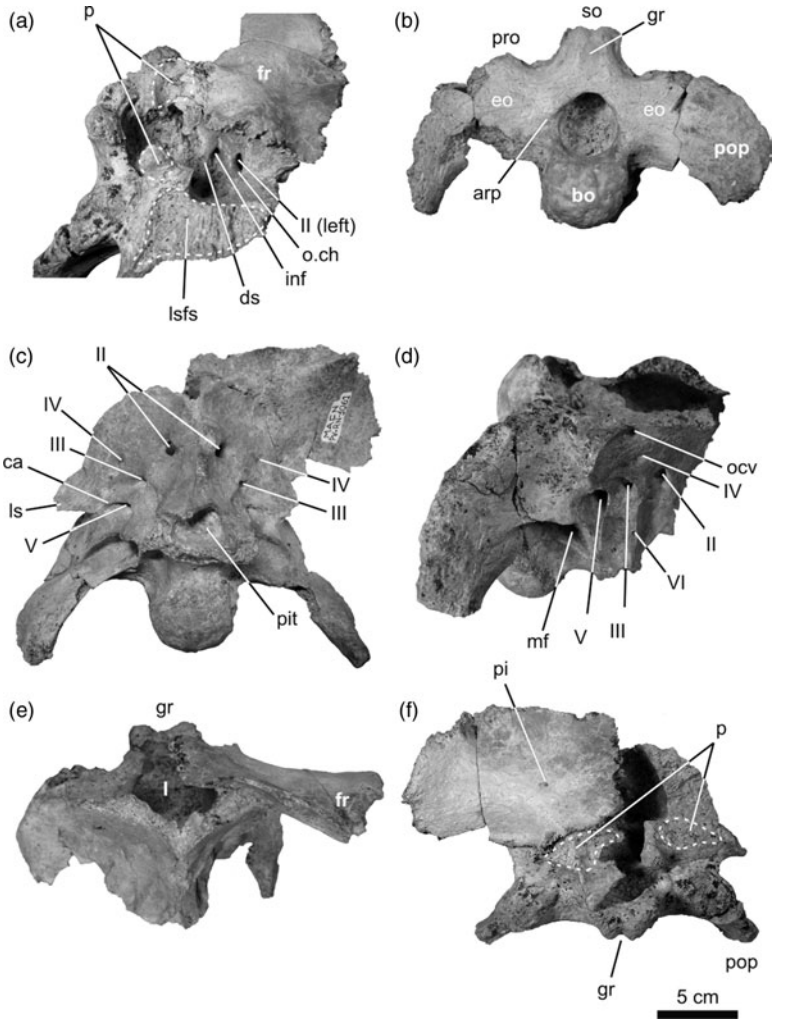

Figure 3. *B. reigi*. MACN-PV RN 1061. Braincase in right dorsolateral (a), posterior (b), anteroventral (c), right lateral (d), anterodorsal (e) and dorsal (f) views. Abbreviations: arp, articulation for the proatlas; bo, basioccipital; ca, crista antotica; ds, dorsum sellae; eo, exoccipital; fr, frontal; gr, groove; inf, infundibulum; ls, laterosphenoid; lsfs, laterosphenoid-frontal suture; mf, metotic foramen; o.ch, optic chiasma; ocv, orbitocerebral vein; p, parietal; pi, pit; pit, pituitary fossa; pop, paroccipital process; pro, prominence; so, supraoccipital.

2.4 Discussion on the original diagnosis

Martinelli and Forasiepi (2004, p. 274) diagnosed *B. reigi* based on the following combination of characters:

(1) longitudinal groove located on the suture between the parietals that continues posteriorly over the supraoccipital to the foramen magnum; (2) basisphenoid tubera long and narrow (more than twice as long as wide); (3) dorsal to middle caudal vertebrae with deep oval to circular pits on both sides of the prespinal lamina; (4) anterior caudal vertebra with spino-postzygapophyseal and spino-prezygapophyseal laminae; (5) neural arch of anterior caudals with deep interzygapophyseal fossae with numerous pits; (6) anterior caudal vertebra with an accessory subhorizontal lamina extending from the anteroventral portion of the postzygapophysis to the mid-portion of the spino-prezygapophyseal lamina and (7) anterior caudal vertebra with a prominent axial crest on the ventral surface of the centrum. (This last character is the only autapomorphy of *Bonatitan*.)

Regarding character 1, we must say that the extension of the groove into the parietals is not corroborated in this study and is excluded from the emended diagnosis (besides, the groove onto the supraoccipital is present in a wide spectrum of sauropods: *Quaesitosaurus*, *Rapetosaurus*, *Saltasaurus* and MML-4). Regarding character 2, the mentioned authors surely refer to the basal tubera, formed mainly by the basioccipital, which is only preserved on the left side of the specimen MACN-PV RN 821. We consider that the ratio (length/width) of the

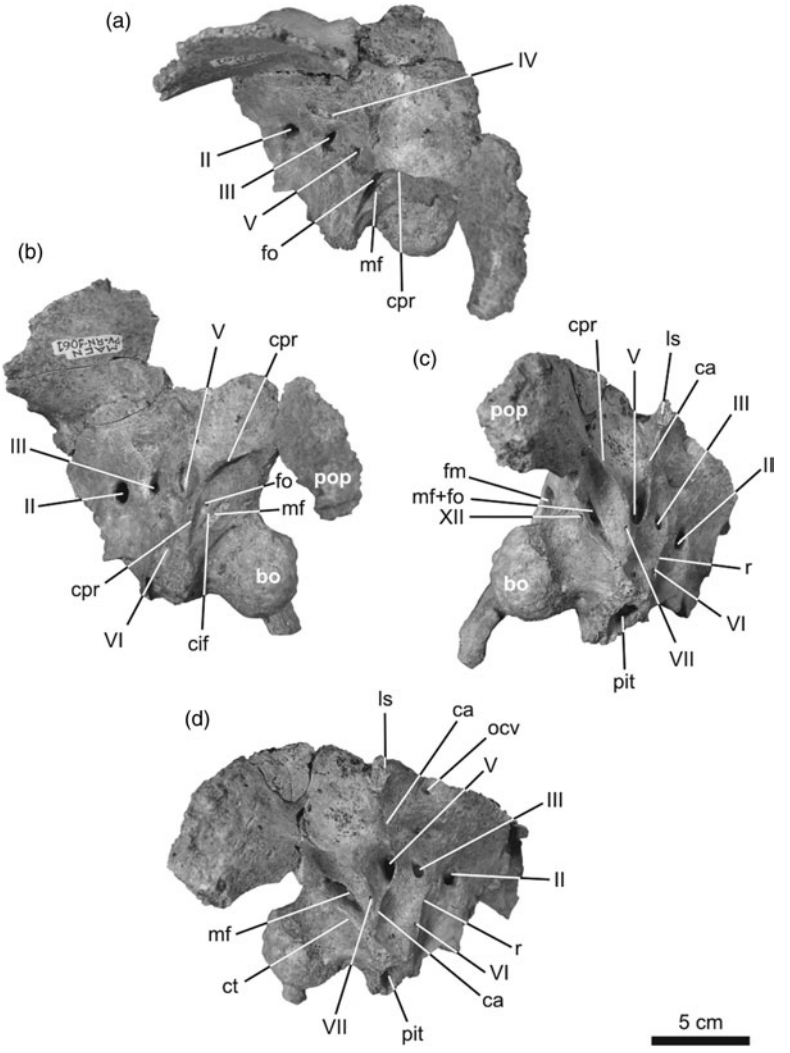

Figure 4. *B. reigi*. MACN-PV RN 1061. Braincase in left lateral (a), left ventro-posterolateral (b), right ventro-posterolateral (c) and right ventrolateral (d) views. Abbreviations: bo, basioccipital; ca, crista antotica; cif, crista interfenestralis; cpr, crista prootica; ct, crista tuberalis; fm, foramen magnum; fo, fenestra ovalis; ls, laterosphenoid; mf, metotic foramen; ocv, orbitocerebral vein; pit, pituitary fossa; pop, paroccipital process; r, rim.

basal tuber is 2:1 (slightly more than twice the width). The same ratio is present in *Saltasaurus* (although slightly shorter) but is 1:1 in most titanosaurs (e.g. *Antarctosaurus*, *Nemegtosaurus*, *Pitekunsaurus* and the unnamed titanosaurs MUCPv-334 and MML 194). Also, considering the length of the basal tubera (from the ventral border of the occipital condyle) relative to the height of the foramen magnum, the development of the basal tubera in *Bonatitan* and *Saltasaurus* is approximately 30% longer than in the mentioned titanosaurs, which would confirm the statement of this character.

2.5 Emended diagnosis

The present study recognised a series of characters that allow enlarging the original diagnosis (characters 1 and 8). The emended diagnosis of *B. reigi* is as follows: (1) small paired pits on the frontals; (2) basisphenoid tubera long and narrow (slightly more than twice as long as wide); (3) dorsal to middle caudal vertebrae with deep oval to circular pits on both sides of the prespinal lamina; (4) anterior caudal vertebra with spino-postzygapophyseal and spino-prezygapophyseal laminae; (5) neural arch of anterior caudals with deep interzygapophyseal fossae with numerous pits; (6) anterior caudal vertebra with an accessory sub-horizontal lamina extending from the anteroventral portion of the postzygapophysis to the mid-portion of the spino-prezygapophyseal lamina; (7) anterior caudal vertebra with a prominent axial crest on the ventral surface of the centrum and (8) posterior ridge of the metacarpal IV.

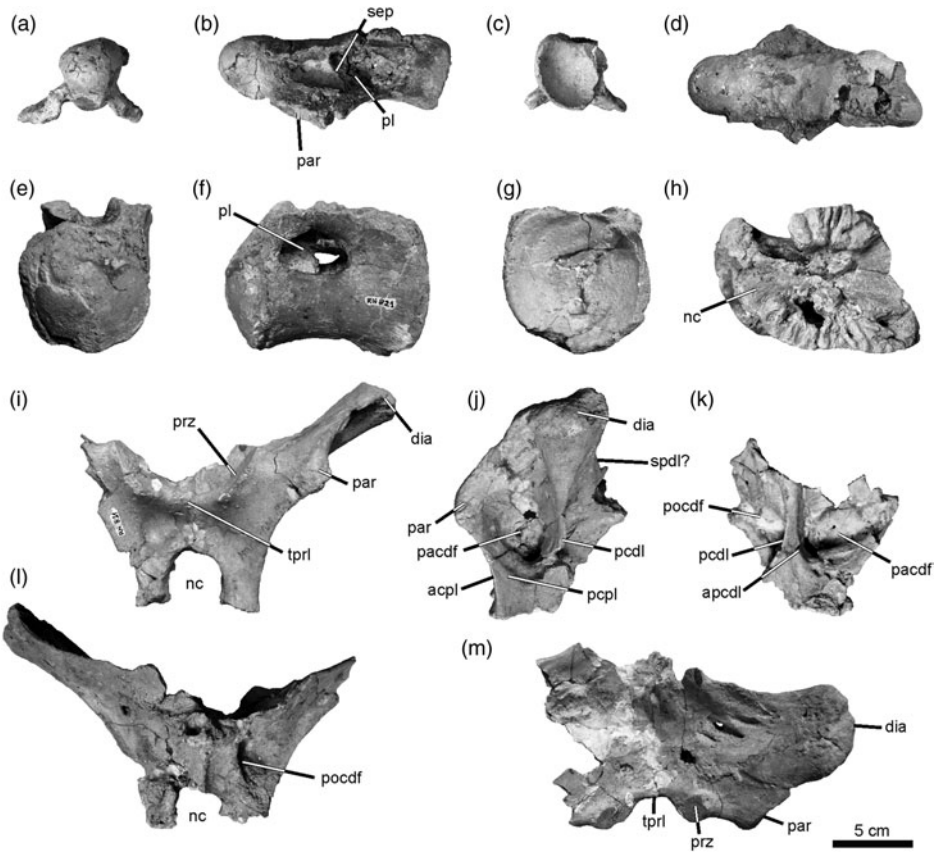

Figure 5. *B. reigi*. MACN-PV RN 1061. Cervical centrum in anterior (a), left lateral (b), posterior (c) and dorsal (d) views. MACN-PV RN 821. Dorsal centrum in anterior (e), left lateral (f), posterior (g) and dorsal (h) views. Mid-dorsal neural arch in anterior (i), left lateral (j), right lateral (k), posterior (l) and dorsal (m) views. Abbreviations: acpl, anterior centroparapophyseal lamina; apcdl, accessory posterior centrodiapophyseal lamina; dia, diapophysis; nc, neural canal; pacdf, parapophyseal centrodiapophyseal fossa; par, parapophysis; pcdl, posterior centrodiapophyseal lamina; pcpl, posterior centroparapophyseal lamina; pl, pleurocoel; pocdf, postzygapophyseal centrodiapophyseal fossa; prz, prezygapophysis; sep, septum; spdl, spinodiapophyseal lamina; tprl, intraprezygapophyseal lamina.

3. Description

All the materials studied by Martinelli and Forasiepi (2004) are redescribed, paying special attention to those features superficially described by those authors, or of which we have a different interpretation. Furthermore, all undescribed materials are included, together with those absent in the original list. Measurements are provided only for the materials published for the first time; measurements of the other bones are indicated in Martinelli and Forasiepi (2004).

3.1 Skull

The description of the skull of *B. reigi* by Martinelli and Forasiepi (2004) was based mainly on the holotype specimen MACN-PV RN 821, although inserting observations on the other specimen. Here, we will follow basically the same criterion, although expanding references to MACN-PV RN 1061.

Both braincases have preserved basically the same elements (Figs 1–4). The individual B (included originally in specimen MACN-PV RN 1061) (Figs 3 and 4) has only its left frontal, lacking most of the parietals, except for some fragments (Fig. 3(a),(f)). Martinelli and Forasiepi (2004) indicate that specimen MACN-PV RN 821 is larger than MACN-PV RN 1061; we interpret exactly the opposite. In the braincase originally assigned to the specimen MACN-PV RN 821, nevertheless, the sutures are less visible than in MACN-PV RN 1061, as Martinelli and Forasiepi (2004, p. 274) emphasise, which suggests that, in spite of its lesser size, the braincase assigned to specimen MACN-PV RN 821 corresponds to an older specimen.

There are minor morphological differences between both braincases. In MACN-PV RN 1061, the supraoccipital

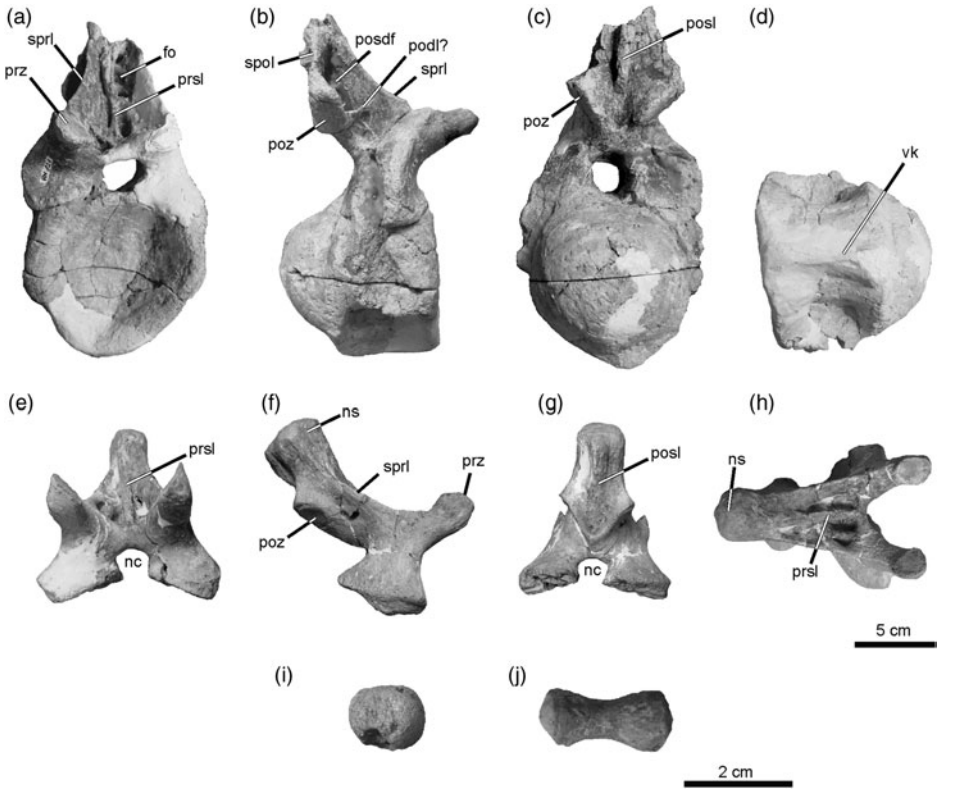

Figure 6. *B. reigi*. MACN-PV RN 821. Anterior caudal vertebra in anterior (a), right lateral (b), posterior (c) and ventral (d) views. MACN-PV RN 821. Mid-caudal neural arch in anterior (e), right lateral (f), posterior (g) and dorsal (h) views. Unnumbered distal caudal vertebra in anterior/posterior (i) and lateral (j) views. Abbreviations: fo, fossa; nc, neural canal; ns, neural spine; podl, postzygodiapophyseal lamina; posdf, postzygapophyseal spinodiapophyseal fossa; posl, postspinal lamina; poz, postzygapophysis; prsl, prespinal lamina; prz, prezygapophysis; spol, spinopostzygapophyseal lamina; sprl, spinoprezygapophyseal lamina; vk, ventral keel.

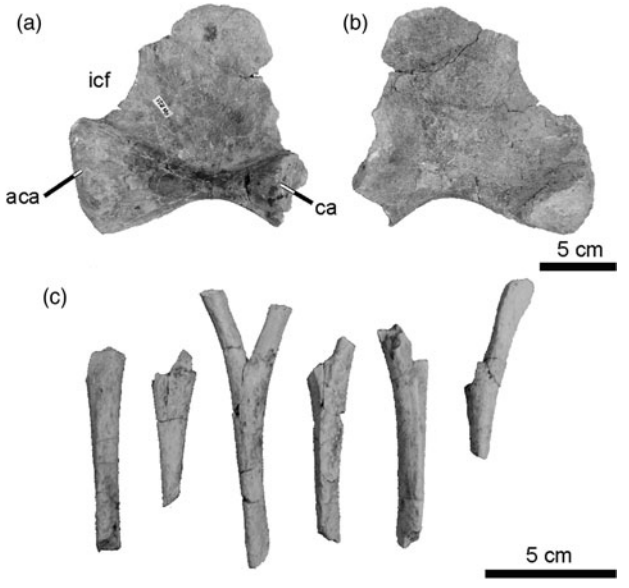

Figure 7. *B. reigi*. MACN-PV RN 821. Right sacral rib in anterior (a) and posterior (b) views. Unnumbered chevrons in anterior (c) views. Abbreviations: aca, acetabular arm; ca, capitulum; icf, intracostal fenestra.

crest is slightly higher, the foramen magnum is wider, the occipital condyle is, seemingly, wider (all this in absolute terms), and the paroccipital processes more robust and a less expanded laterally. The neck of the occipital condyle is nearly parallel to the skull roof in MACN-PV RN 1061, whereas it is more projected ventrally in MACN-PV RN 821. In this last specimen, there is a small foramen dorsally to the *fenestra ovalis*, which is absent in the other specimen; it is probably a vascular element related to the dorsal head vein. In the specimen MACN-PV RN 1061, the bony ridges seem to be sharper than in the holotype specimen.

For descriptive purposes, the skull will be oriented with the occipital plate vertical, and the occipital condyle pointing posteroventrally (Martinelli and Forasiepi 2004 had oriented the condyle posteriorly, with the occipital plate inclined anterodorsally). This orientation is obtained when the neurocranium is disposed with the lateral semicircular canal of the inner ear parallel to the ground (Paulina Carabajal 2012).

Figure 8. *B. reigi*. MACN-PV RN 821 (individual D). Left humerus in posterior (a), anterior (b), distal (c) and dorsal (d) views. Abbreviation: af, anconeal fossa.

3.1.1 Frontal

The frontals are wider than long, as in most sauropods (Figures 1(b),(d) and 3(a),(e),(f)). The interfrontal suture is clear, more anteriorly than posteriorly (Figure 1(b),(d)). Martinelli and Forasiepi (2004) report that the frontals of *Bonatitan* are not fused, as in most sauropods. In fact, the frontals tend to remain unfused in dinosaurs (or, at least, the interfrontal sutures are normally visible), whereas the parietals are fused in very early ontogenetic stages (APC personal observation).

There is a median protuberance near the anterior margin of the frontals (Figure 1(b)), as in *Saltasaurus*, *Antarctosaurus*, *Rapetosaurus* and specimen MGPIFD-GR 118 (Powell 2003; Curry Rogers and Forster 2004; Paulina Carabajal and Salgado 2007), although less developed dorsally. Laterally to this prominence, there are distinct pits in both specimens (Figures 1(b),(d) and 3 (f)). There is no internal communication of these foramina with the endocranial cavity, and is not possible to determinate whether correspond to vascular foramina. This pair of foramina has not been identified in other titanosaur frontals.

Martinelli and Forasiepi (2004) stated that the frontals of *B. reigi* are fused to the parietals. However, a sutural contact with the parietals is distinguishable through the nuchal crest (Figure 1(b),(d)). On the midline, between parietals and frontals, there is a circular median depression

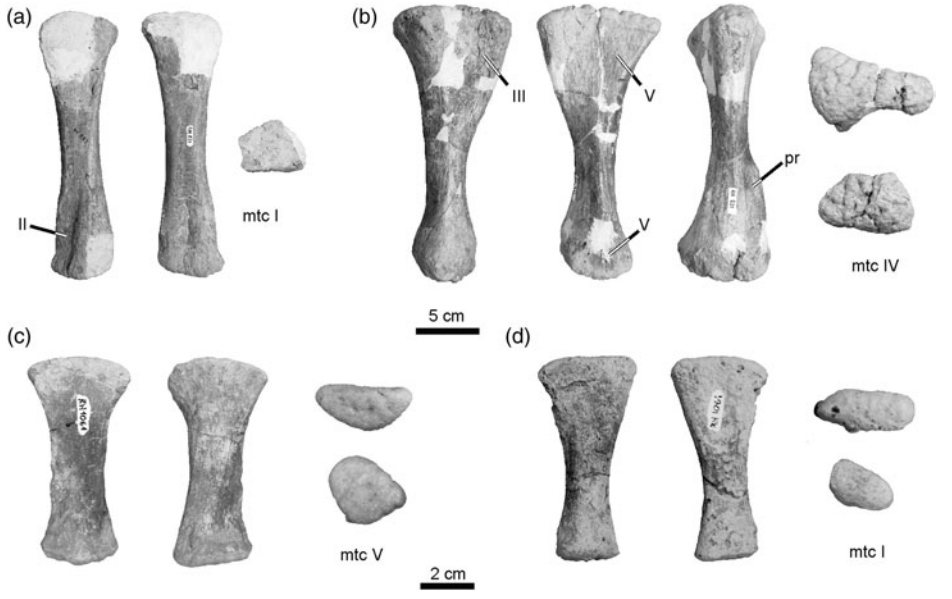

Figure 9. *B. reigi*. MACN-PV RN 821. (a) Left metacarpal I in medial, lateral and distal views (individual A); (b) right metacarpal IV in anterior, posterior, medial, proximal and distal views (individual A). MACN-PV RN 1061; (c) right metacarpal V in anterior, posterior, proximal and distal views (individual E); (d) right metacarpal I in medial, lateral, proximal and distal views (individual E). Abbreviation: pr, posterior ridge.

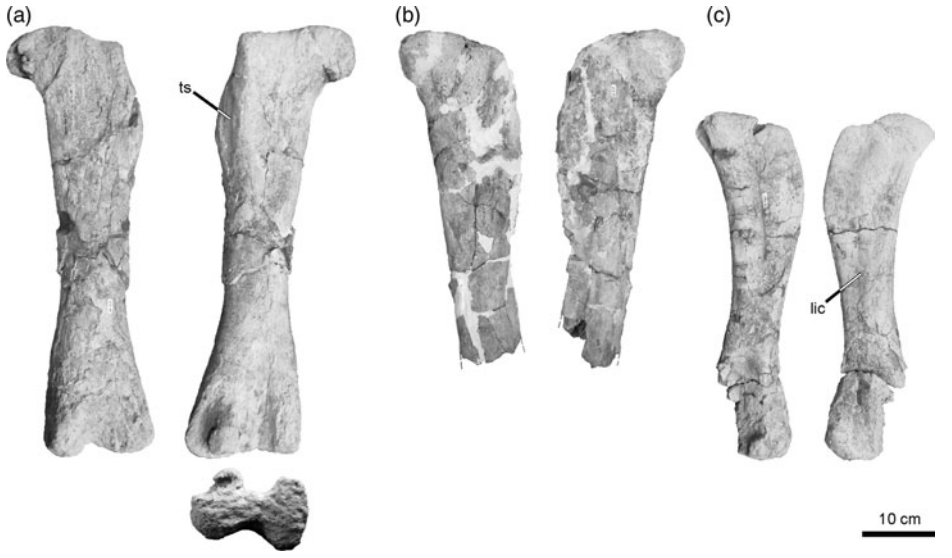

Figure 10. *B. reigi*. MACN-PV RN 821. (a) Left femur in anterior, posterior and distal views (individual B); (b) right femur in posterior and anterior views (individual B). MACN-PV RN 1061. (c) Right femur in posterior and anterior views (individual D). Abbreviations: lic, linea intermuscularis cranialis; ts, trochanteric shelf.

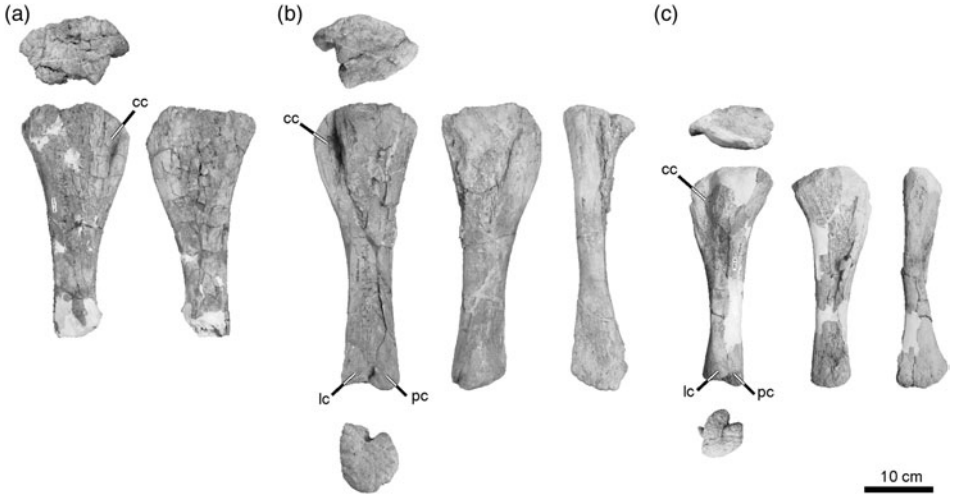

Figure 11. *B. reigi*. MACN-PV RN 821. (a) Right tibia in lateral, medial and dorsal views (individual A); (b) left tibia in lateral, medial, anterior, proximal and distal views (individual B). MACN-PV RN 1061. (c) Left tibia in lateral, medial, anterior, proximal and distal views (individual D). Abbreviations: cc, cnemial crest; lc, lateral condyle; pc, posterior condyle.

(Figure 1(d)) that corresponds with the non-ossified space present in other titanosaurs, as in specimen MGPIFD-GR 118.

The orbital margin of the frontal of *B. reigi* is rounded and laterally projected (Figure 1(e),(f)). In other titanosaurs (e.g. *Nemegtosaurus mongoliensis*, *Antarctosaurus wichmannianus* and *Rapetosaurus krausei*) and in diplodocoids (e.g. *Amargasaurus cazaui*, *Limaysaurus tessonei* and *Diplodocus longus*), the lateral margin of the frontal is rather sigmoid, showing a main posterior lobe that is convex and superficial in *Nemegtosaurus* and *Saltasaurus*, oblique in *R. krausei* and *Phuwiangosaurus sirindhornae*, and strongly expanded in *B. reigi*. In contrast, in *Bonitasaura*, it is straight throughout all its extension, without evidence of a lobe, as in the specimen MGPIFD-GR 118 (Paulina Carabajal and Salgado 2007).

Martinelli and Forasiepi (2004) stated that in *Bonatitan* the frontals participate of the supratemporal fenestra, 'like in *Antarctosaurus*, *Rapetosaurus* and *Saltasaurus*'. However, the condition differs in these three genera. In fact, the contribution of the frontal to the supratemporal fenestra is minimal in *Antarctosaurus*, being practically null in *Bonitasaura*. In turn, in *Saltasaurus* (PAG personal observation) and *Nemegtosaurus*, the frontal is completely

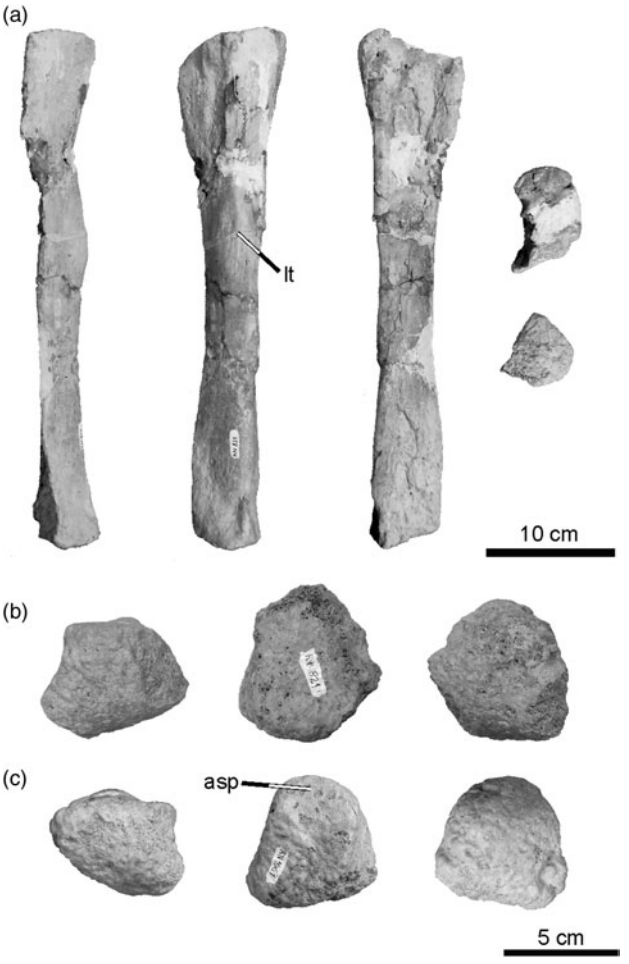

Figure 12. *B. reigi*. MACN-PV RN 821. (a) Left fibula in anterior, lateral, medial, proximal and distal views. MACN-PV RN 821. (b) Right astragalus in anterior, dorsal and ventral views (individual B). MACN-PV RN 1061. (c) Left astragalus in anterior, dorsal and ventral views (individual D). Abbreviations: lt, lateral trochanter, asp, ascending process.

excluded from the supratemporal fenestra (against Curry Rogers and Forster 2001). The opposite condition is observed in *Rapetosaurus*, MGPIFD-GR 118, and *Bonatitan*, in whom the absence of an anteromedial projection of the parietal allows the participation of the frontal in the supratemporal fenestra (Figures 1(b)–(e) and 2(b)).

The contact of the frontal with the lateral wall of the neurocranium (laterosphenoids, orbitosphenoids and sphenethmoids) is sutural. The frontals roof anteriorly the anteroposteriorly short cavity in which the olfactory bulbs lodged (Figure 2(b),(e)) and left their impression on the ventral aspect of each frontal (Paulina Carabajal 2012). These impressions are oval and slightly divergent, and are bounded lateroventrally by two small sphenethmoids (Figure 2(b),(e)).

3.1.2 *Parietals*

Both parietals are complete in the specimen MACN-PV RN 821. These are anteroposteriorly short elements (Figure 1(b)–(d)). The interparietal suture is unclear, and the nuchal crest is low but well marked (Figure 1(d)). The posterolateral wing of each parietal leans on the paroccipital process contacting the exoccipital–opistotic complex (Figure 1(c),(d)).

3.1.3 *Supraoccipital*

The supraoccipital is a vertical element in the occipital table of specimen MACN-PV RN 821, but it is posteroventrally inclined in MACN-PV RN 1061. The supraoccipital prominence presents a median groove (Figures 1(a),(b) and 3(b),(e),(f)). According to Martinelli and Forasiepi (2004), this groove extends onto the parietal, which would be a characteristic of *B. reigi* (character '1' of their diagnosis). However, it is not clear that the furrow extends towards the parietal in this species: in this bone there is certainly a depression (Figure 1(b),(d)), but it does not seem to be continuous with the supraoccipital groove. Clearly, the furrow of the supraoccipital is present in *Saltasaurus loricatus*, although Martinelli and Forasiepi (2004) do not mention it, and in the specimen MML 194 (García et al. 2008), as well as in *Quaesitosaurus* (Kurzanov and Bannikov 1983) and *Rapetosaurus*, as Martinelli and Forasiepi (2004) recognise. However, the furrow is absent in the unnamed titanosaurs MUCPv 334 (Calvo and Kellner 2006), MGPIFD-GR 118 (Paulina Carabajal and Salgado 2007), *Pitekunsaurus* (MAU-Pv-AG 446/5), *Antarctosaurus* (as Martinelli and Forasipei (2004) recognise), *Narambuenatitan* (Filippi et al. 2011), *Nemegtosaurus* (Wilson 2005) and *Jainosaurus* (Wilson et al. 2009).

The supraoccipital forms the dorsal margin of the foramen magnum, which is higher than wide (Figure 1(a)). In the specimen MACN-PV RN 1061, the foramen is suboval and lower than in the holotype (Figure 3(b)). The laterodorsal protuberances to both sides of the foramen magnum would be indicating the exoccipital–supraoccipital contact (Figures 1(a) and 3(b)).

3.1.4 *Exoccipital–opistotic complex*

The paroccipital processes project laterally, and their distal ends reach (surpass in the case of the right paroccipital process of the specimen MACN-PV RN 821) the level of the ventral border of occipital condyle (Figures 1(a),(e),(f), 3(b),(d) and 4). The dorsal edge of each process presents a protuberance that contact anteriorly with the parietal. This protuberance generates two depressions, lateral to the supraoccipital prominence (Figures 1(a),(d) and 3(b)). The exoccipital forms the

Figure 13. *B. reigi*. MACN-PV RN 1061. (a) Left metatarsal I in lateral, medial, proximal and distal views (individual A). MACN-PV RN 821. (b) Right metatarsal III in lateral, medial and proximal views (individual A); (c) unnumbered metatarsal V in lateral and medial views (individual A); (d) unnumbered metatarsal I in dorsal and proximal views (individual D); (e) unnumbered metatarsal III in dorsal, ventral and distal views (individual D); (f) unnumbered metatarsal V in lateral, medial and proximal views (individual D); (g) unnumbered metatarsal V in lateral, medial and distal views (individual D). MACN-PV RN 1061. (h) Metatarsal III? in lateral, medial, proximal and distal views (individual D); (i) unnumbered ungueal phalanx in lateral, medial and proximal views (individual D).

lateral margins of the foramen magnum (Figures 1(a) and 3(b)). The protuberances for the contact with the proatlas would be indicating the exoccipital–supraoccipital contact ('arp' in Figures 1(a) and 3(b)). These paired prominences are less developed in the specimen MGPIFD-GR118 (Paulina Carabajal and Salgado 2007) and in *Antarctosaurus* (Powell 2003).

Laterally to the occipital condyle, there is a single foramen for the branches of the CN XII (Figures 1(c), 2(d) and 4(c)) like in most titanosaurs, with the exception of *Pitekunsaurus* (Paulina Carabajal 2012) and *Rapetosaurus* (Curry Rogers and Forster 2004). In these two taxa, there is also a single foramen externally, but they have two openings endocranially.

The metotic foramen (for cranial nerves IX–XI) is delimited posteriorly by the exoccipital and anteriorly by the opisthotic (Figures 1(f), 2(a),(c), 3(d) and 4(a)–(d)). It is large, oval and opens anteriorly within a broad oval recess delimited between the *crista prootica* anteriorly, and a ventral branch of the opistotic that forms the ventral edge of the paroccipital process posteriorly (the *crista tuberalis*) (Figures 2(c) and 4(d)). Within the same recess opens also the foramen ovalis, which is smaller, and is separated from the metotic foramen by a thin septum of bone (the *crista interfenestralis*, Figures 2(c) and 4(b)).

The occipital condyle is formed mainly by the basioccipital, although the sutures between this element and the exoccipitals are not clear. The dorsal rim of the condyle is flat, and is not circular in posterior view (Figures 1(a) and 3(b)).

In *Bonatitan*, like in other titanosaurs, the CN VII is located rostrally to the *fenestra ovalis*, on the edge of the

crista prootica (Figures 1(f) and 2(a),(c),(d)). In *Saltasaurus*, it is not exactly on the edge, but rostral or caudal to it (García et al. 2008).

3.1.5 *Basioccipital*

Martinelli and Forasiepi (2004) stated that the occipital condyle of *Bonatitan* was normally oriented posteriorly, as in *Rapetosaurus*. However, when the condyle is posteriorly oriented in the Patagonian sauropod, the basipterygoid processes would not have been oriented anteroventrally, as Martinelli and Forasiepi (2004, p. 276) interpret, but posteroventrally. When the neurocranium of *Bonatitan* is oriented with the lateral semicircular canal of the inner ear horizontal (Paulina Carabajal 2012), the occipital plate is vertical, the occipital condyle is posteroventrally oriented and the basipterygoid processes are anteroventrally projected (Figure 1(e),(f)). This orientation would have been habitual in *Bonatitan*. Indeed, the direction of the condyle is unusual in *Rapetosaurus*; as it is shown by Curry Rogers and Forster (2004, Fig. 23), the condyle of this genus is posteriorly oriented and the basipterygoid processes anteroventrally projected.

In *Bonatitan*, the basal tubera are relatively longer than in *Rapetosaurus*, *Antarctosaurus*, *Muyelensaurus*, *Nemegtosaurus* and MML-194 (Figures 1(a) and 2(b)–(d)). In the African genus, the angle of divergence of the tubera is greater than that formed by the basipterygoid processes, as in *Antarctosaurus*; in *Bonatitan*, in contrast, the angle is equal (Figure 1(a)). In *Bonatitan*, the basal tubera are formed mainly (if not only) by the basioccipital.

In the braincase MACN-PV RN 1061, the occipital condyle seems to be more horizontal than in MACN-PV RN 821. In turn, the condyle of MACN-PV RN 1061 is larger and has a rougher surface. The neck of the condyle is more robust in MACN-PV RN 1061 than in the holotype. García et al. (2008) report that the relative size of the foramen magnum and occipital condyle is equal in *Bonatitan* and the braincase MML-194 (the foramen magnum being a 25% higher than the condyle; 26 mm against 20 mm). In *Lirainosaurus*, the foramen magnum is wider than the occipital condyle (Díez Díaz et al. 2011). In other sauropods (and, among titanosaurs, in *Quaesitosaurus* and *Nemegtosaurus*), the condyle is higher than the foramen magnum (Paulina Carabajal 2012).

3.1.6 *Basisphenoid*

The basisphenoid is the main component of the basicranium and forms the floor of the endocranial cavity. It is firmly fused to the basioccipital posteriorly, and to the prootics and laterosphenoids dorsally. The basipterygoid processes are long and lateromedially compressed (Figures 1(a),(e),(f) and 2(a)–(e)). They project anteroventrally when the occiput is oriented vertically. The distal end of the basipterygoid process is slightly expanded anteroposteriorly (Figures 1(e),(f) and 2(a),(e)). The proximal sector of the processes is fused posteriorly. The shape of the lamina that connects both processes seems to have taxonomic value, but it is not preserved in *B. reigi*. Like in other titanosaurs, the foramen of the internal carotid artery opens in the medial side of the basipterygoid process (Figures 1(c),(e) and 2(a)), reason by which it is not observed in lateral view (Paulina Carabajal 2012). The foramen indicated as 'carotid foramen' by Martinelli and Forasiepi (2004, Figs 7 and 8) is, in fact, the CN VI. The carotid penetrates the pituitary fossa posteroventrally. This is a cavity that projects posteroventrally within the basisphenoids (Figures 1(c) and 3(c)). Two pairs of vascular foramina pierce this fossa (Paulina Carabajal 2012). In front of it, a fragment of the base of the cultriform process is preserved, which is formed by the parasphenoid (Figures 1(e) and 2(b),(c),(e)). The CN VI leaves the endocranial cavity through a small foramen located behind the dorsum sellae (Figures 1(e),(f), 2(a)–(c), 3(d) and 4(b)–(d)); laterally, it crosses the basisphenoid, lateral to the pituitary fossa, to emerge through a foramen located ventral to CN V. As said above, Martinelli and Forasiepi (2004) indicate erroneously as 'carotid foramen' (Caf) the CN VI (Martinelli and Forasiepi 2004, Figs 7 and 8). Dorsally to CN VI, there are two pituitary foramina (the dorsal one is erroneously indicated as CN VI by Martinelli and Forasiepi 2004, Figs 7 and 8) (Figures 1(f) and 2(b),(c)).

3.1.7 *Prootic*

The prootic is firmly fused to the opistotic posteriorly, to the laterosphenoid anteriorly and to the basisphenoid ventrally. Dorsally, the contact with the frontal is a clear suture (Figure 2(c),(d)). Cranial Nerve V, which is delimited posteriorly by the prootic, is large and oval-shaped (Figures 1(e),(f), 2(a)–(c), 3(c),(d) and 4(a)–(d)). Martinelli and Forasiepi (2004, p. 287) mentioned that CN V is particularly large in titanosaurs, except in *Quaesitosaurus* (Kurzanov and Bannikov 1983). It is delimited anteriorly by a low and poorly pronounced crest, the *crista antotica* (formed by the laterosphenoid) (Figures 1(f), 2(a)–(d) and 4(c),(d)), and posteriorly by the *crista prootica* (Figures 1(f), 2(a),(c),(d) and 4(a)–(c)), which is markedly projected laterally, being visible in posterior view. Martinelli and Forasiepi (2004, p. 277) mention a furrow for the maxillary branch of the CN V (CN V_2) that would reach the basipterygoid processes, but they did not show it in the corresponding figures. This furrow runs ventrally from CN V (Figure 1(f)).

Cranial Nerve VII exits posteroventrally to the CN V, on the ventral sector of the *crista prootica* (Figures 1(f), 2

(a),(c),(d) and 4(c),(d)). There is also a ventrally projected groove related to this foramen that corresponds to the palatine branch of this nerve.

3.1.8 *Laterosphenoid–orbitosphenoid*

There are no visible sutures between laterosphenoid and orbitosphenoid. The laterosphenoid forms a robust postorbital process, the *crista antotica*, which is posterolaterally projected (Figures 1(c),(e),(f), 2(a)–(d), 3(c) and 4(c),(d)). This process delimits anteriorly the small supratemporal fossa (Figure 1(c),(e)). The laterosphenoid forms the posterior margins of the openings for the CN III and CN IV (Figures 1(f), 2(a)–(d) and 3(c)). The foramen for CN III is larger than CN IV and opens anteriorly to CN V, whereas CN IV opens dorsally to CN III. Dorsally to CN III and IV, and in front of the base of the *crista antotica*, there is a small vascular foramen near the contact of the laterosphenoid with the frontal (Figures 1(f), 2(b) and 4(d)). This foramen corresponds to the orbitocerebral vein (Paulina Carabajal 2012), not indicated by Martinelli and Forasiepi (2004). The orbitosphenoids contact to each other ventromedially, delimiting the foramina for CN II. Cranial Nerve II leaves the endocraneal cavity through separated circular foramina (Figures 1(e),(f), 2(a)–(e), 3(a),(c),(d) and 4(a)–(d)). In the specimen MACN-PV RN 821, the CN III has half of the size of CN II; in the specimen MACN-PV RN 1061, CN III is relatively greater (two-thirds of CN II). Martinelli and Forasiepi (2004, p. 287) stated that the exit for CN II is especially large in titanosaurs (*Bonatitan*, *Saltasaurus*, *Quaesitosaurus* and *Rapetosaurus*), unlike other neosauropods. However, other macronarians, such as *Camarasaurus*, and dicraeosaurids also have large CN II foramina. Besides, they say (p. 277) that in non-titanosaur sauropods (e.g. *Camarasaurus* and diplodocoids), CN II and CN III are almost equal in size.

In MACN-PV RN 1061, on both sides, dorsal to the foramen for CN III, there is a rim that Martinelli and Forasiepi (2004) do not describe that is not visible in MACN-PV RN 821. This rim is developed on the suture between the laterosphenoid and the orbitosphenoids and is parallel to the *crista antotica*, which is located anteriorly (Figure 4(c),(d)). Perhaps, this rim results of the relatively greater size of the foramen for CN III in the specimen MACN-PV RN 1061; perhaps, it is simply the result of the impression left by vascular soft tissue. The 'mesencefalic vein' mentioned by Martinelli and Forasiepi (2004, p. 276) is not indicated in their figures. It seems to have been drawn between the laterosphenoid and frontal (Martinelli and Forasiepi 2004, Figs 7 and 8). In fact, the drawn foramen would be the orbitocerebral vein (Paulina Carabajal 2012) (Figures 1(f), 2(b), 3(d) and 4(d)).

3.1.9 *Ethmoidal elements*

Fragments of ethmoidal elements (probably the sphenethmoids) are preserved in contact with the frontals dorsally and the orbitosphenoids posteriorly, delimiting laterodorsally the short olfactory tract and the cavity for the olfactory bulbs. The impressions of the small olfactory bulbs are in the ventral aspect of the frontals (Figure 2(b),(e)).

3.2 *Postcranial axial skeleton*

3.2.1 *Cervical vertebrae*

Only one cervical centrum is preserved (Figure 5(a),(b)). Martinelli and Forasiepi (2004) stated, on the basis of its relatively small size, that it pertains to the specimen MACN-PV RN 1061, but here we consider that it belongs to the individual B (see above). Martinelli and Forasiepi (2004) also interpreted that this element is an anterior cervical, although they did not explain why. Considering other titanosaurs, such as *Rapetosaurus* or *Alamosaurus* (Lehman and Coulson 2002), the preserved centrum of *Bonatitan* could be, instead, a posterior cervical. In fact, proportionally, this is similar to the cervical 14 of *Rapetosaurus* (Curry Rogers 2009, Figure 11B–D), although in the last genus the posterior articulation is inclined in lateral view, whereas in *Bonatitan* is rather straight.

The centrum is long and sub-cylindrical, not dorsoventrally depressed as in *Saltasaurus*, *Neuquensaurus* or *Trigonosaurus* (Campos et al. 2005). The parapophyses project more latero-ventrally than laterally (Figure 5(a),(c)), like in *Saltasaurus* and *Neuquensaurus*. The Elongation Index of *Bonatitan reigi* (centrum length/width of the posterior articulation) is 2.54 (length: 12.2 cm; estimated width of the posterior articulation: 4.8 cm), whereas in *Rapetosaurus krausei* it is from 3.3 to 4.3 (in the Malagasy genus, the anterior cervicals seem to have the lowest index). In *Pitekunsaurus* (Filippi and Garrido 2008, Fig. 2), the Elongation Index of the cervical vertebrae varies between 3.5 and 4 (although Filippi and Garrido 2008 do not indicate how the width of the centrum was taken); in *Bonatitan*, therefore, the cervical centra are slightly shorter than in the Neuquenian genus.

In *Bonatitan*, as in *Rapetosaurus*, the pleurocoel is divided by an oblique *septum*. Nevertheless, the direction of that *septum* is different in both genera: from the anterodorsal up to the posterior-ventral corner of the pleurocoel in *Bonatitan*; and from the anteroventral up to the posterior-dorsal in *Rapetosaurus*. The parapophyses of the cervical centrum of the Patagonian sauropod are posterior with respect to the position that occupy in the Malagasy sauropod, as observed in ventral view (Curry Rogers 2009, Fig. 7D,E).

In *Rapetosaurus*, the neural pedicels of the cervical centrum are constricted right above the level of the parapophyses. According to Curry Rogers (2009), that constriction, which persists throughout the cervical series, reduces the participation of the centrum from the neural canal. The constriction is actually present in *Uberabatitan* (Salgado and Carvalho 2008, Fig. 4A) and *Bonitasaura* (MPCA 460); in *Alamosaurus* is also observed, at least in juvenile specimens (Lehman and Coulson 2002). In the North American genus, the constriction seems to be more pronounced in the mid than in the anterior cervical (Lehman and Coulson 2002, Fig. 2). This constriction is not observed in *Rocasaurus* (Salgado and Azpilicueta 2000, Fig. 2). In *Bonatitan*, the cervical pedicels are not very well preserved, but they seem to have had a constriction, mainly from what is observed on the right side.

3.2.2 *Dorsal vertebra*

The only dorsal centrum preserved (Figure 5(e)–(h)), possibly a posterior dorsal, is relatively higher than those of *Alamosaurus*, *Trigonosaurus* and *Rapetosaurus*, and decidedly shorter than those of *Lirainosaurus* (Diez Díaz et al. 2013a). It has a broad pleurocoel, anteriorly located (Figure 5(f)), more than in *Neuquensaurus*, where it occupies most of the lateral face of the centrum, as in *Rapetosaurus*. In *Rapetosaurus* and *Lirainosaurus*, the pleurocoels are acuminate both anteriorly and posteriorly, whereas in *Bonatitan* these are poorly acuminate, anteriorly, and non-acuminate, posteriorly.

The only neural arch preserved in *B. reigi* (Figure 5 (i)–(m)) is similar to the fifth dorsal of *Rapetosaurus* (Curry Rogers 2009, Fig. 18). In this sense, we agree with the allocation proposed by Martinelli and Forasiepi (2004), which consider the vertebra as a mid-dorsal.

The neural canal of the mid-dorsal of *Bonatitan* is relatively large (Figure 5(i),(l)), markedly more than in *Bonitasaura* and *Alamosaurus*; however, as stated above, these two genera are known from juvenile individuals; we ignore if the relatively large neural canal of *Bonatitan* obeys to its youthful condition.

On the left side of the neural arch (Figure 5(j)) is observed that, unlike *Rapetosaurus*, the posterior centroparapophyseal lamina (pcpl) (little developed on this side) does not form an acute angle with the accessory posterior centrodiapophyseal lamina (apcdl, which is not differentiated as a true lamina on the left side), but rather a rounded margin. In other words, in *Bonatitan*, the parapophyseal centrodiapophyseal fossa (pacdf) (Wilson et al. 2011) (the pparf, postparapophyseal fossa of Martinelli and Forasiepi 2004) is ventrally rounded, whereas in *Rapetosaurus* is V-shaped. In *Lirainosaurus*, the pacdf is also rounded, although it does not extend so ventrally as in *Bonatitan*. In general, the neural fossae are deeper in *Rapetosaurus* and *Bonitasaura* than in *Bonatitan*.

On the right side (Figure 5(k)), there is a well-developed apcdl (Martinelli and Forasiepi 2004 illustrate the neural arch only on the left side). On the same side, it is observed that the surface between the pcdl and apcdl is broad and flat. On the left side, this surface is continuous with other, anterior, extended between the pcpl and the anterior centroparapophyseal lamina (acpl). In this sense, in *Bonatitan*, the acpl is not very differentiated from the pcpl (Figure 5(j)); the centroparapophyseal fossa (cpaf) is not present in *Bonatitan*, although on its corresponding site there is a flat, subtriangular surface. In this sense, *Bonatitan* resembles *Lirainosaurus*, where the pcdl has been described as being not 'ventrally bifurcated', which is interpreted by Díez Díaz et al. (2013a) as an autapomorphy of *Lirainosaurus astibiae*.

In *Bonatitan*, the pocdf (the postzygapophyseal centrodiapophyseal fossa) is not markedly deep, and the laminae that limit it are not conspicuous. In *Trigonosaurus*, the apcdl is well developed (Campos et al. 2005), as well as the pocdf and pacdf, as in *Rapetosaurus* and *Neuquensaurus*, and unlike *Bonatitan* and *Lirainosaurus*.

In *Bonatitan*, the space below the intraprezygapophyseal lamina (tprl) and the neural canal is much broader than in the dorsal 4 of *Trigonosaurus* (Campos et al. 2005, Fig. 16), reason by which the neural arch of the mid dorsal seems to be higher in the Patagonian genus (Figure 5(i)). In this sense, *Rapetosaurus* seems to occupy an intermediate position in the sequence (Curry Rogers 2009, Figs 17 and 18).

Martinelli and Forasiepi (2004) mention the existence of a postzygodiapophyseal lamina (podl) in the mid-dorsal neural arch of *Bonatitan*. However, this presence is doubtful, as the referred lamina is probably the spinodiapophyseal lamina (spdl) (Figure 5(j)). Thus, the condition in *Bonatitan* would be as in *Trigonosaurus* (and possibly in *Lirainosaurus*), where the podl appears just in the posterior-most dorsals or even in the last dorsal (Salgado and Powell 2010).

3.2.3 *Sacral rib*

An almost complete right sacral rib has been preserved (Figure 7(a),(b)), which is very similar to the fourth sacral rib of *Rapetosaurus* (Curry Rogers 2009, Fig. 24). It is a laminar bone, with the capitulum subtriangular and the acetabular arm strongly dorsoventrally expanded. On its anterior face is observed that the ventral margin of the sacral rib is thickened and concave, as in *Rapetosaurus*. The rest of the bone is very laminar. Part of the intracostal fenestra can be observed; the preserved sector of this fenestra is a curved edge, closer than in *Rapetosaurus*,

which is probably because the whole rib is shorter. The edge of the transverse foramen is not observed (Wilson 2011). The posterior surface of the sacral rib is practically flat, and the ventral thickening that is observed in the anterior surface is not present here.

3.2.4 Caudal vertebrae

Three caudal vertebrae have been preserved: a complete anterior caudal vertebra, corresponding to the individual A (published by Martinelli and Forasiepi 2004 as MACN-PV RN 821; Figure 6(a)–(d)); a neural arch of a mid caudal (published by those authors as pertaining to specimen MACN-PV RN 821, but interpreted here as part of the individual B; Figure 6(e)–(h)); and a distal caudal, originally undescribed and not numerated (here assigned to specimen E; Figure 6(i),(j)).

The centrum of the anterior caudal is procoelic. On its ventral surface, there is a remarkable keel, which Martinelli and Forasiepi (2004) consider an autapomorphy of *Bonatitan* (Figure 6(d)). The prezygapophyses of the anterior caudal are very short, and the articular facets very reduced, compared with those of other titanosaurs, as aeolosaurines and *Mendozasaurus neguyelap* (González Riga 2003, 2005).

In the anterior caudal of *Bonatitan*, the spinoprezygapophyseal lamina (sprl) seems to be less developed than in *Rapetosaurus*; or, at least, in the Patagonian genus the sprl is more concave in lateral view (Figure 6(b)). In the anterior caudal vertebrae, between the sprl and the anterior margin of the postzygapophysis and the spinopostzygapophyseal lamina (spol), there is the postzygapophyseal spinodiapophyseal fossa (posdf) (the 'interzygapophyseal fossa' of Martinelli and Forasiepi 2004) with a series of foramina that are not present in the anterior caudal of *Rapetosaurus* (Curry Rogers 2009, Fig. 27D) (Figure 6(b)). That fossa seems to be present also in the anterior caudal of *Neuquensaurus* (Salgado et al. 2005), although in this last genus there are not pits. Likewise, in *Bonatitan* and *Neuquensaurus*, there is a series of foramina to both sides of the prespinal lamina (prsl) that are not present in the Malagasy sauropod.

In the anterior caudal vertebra, there is a lamina that Martinelli and Forasiepi (2004) consider as an 'accessory' lamina, but that is here interpreted as a podl, with doubts; a similar lamina is observed in *Neuquensaurus* (Salgado et al. 2005). The anterior caudal has preserved the base of its neural spine, which seems to be anteroposteriorly short.

Contrary to that mentioned by Martinelli and Forasiepi (2004), the anterior edge of the neural spine of the neural arch of mid caudal is not at the level of the posterior margin of the postzygapophyses when the neural canal is oriented horizontally (Figure 6(f)). Precisely, this character is one of the three invocate by Martinelli and Forasiepi (2004) in support of the Saltasaurine affinities of *Bonatitan*. A general description of this vertebra was provided by Martinelli and Forasiepi (2004), and we will not add anything else here.

The distal caudal of the individual E is cylindrical with its ends expanded (Figure 6(i),(j)). Its measurements are as follows: length = 2 cm; width = 1.2 cm; height of the articular face = 1 cm. It is not possible to know which is the anterior face and which is the posterior face. The articular surfaces are slightly convex.

3.2.5 Chevrons

Six fragments of chevrons are preserved (Figure 7(c)). They were not previously described, but mentioned as part of the referred specimen MACN-PV RN 1061 (Martinelli and Forasiepi 2004, p. 274). Because of their size, we interpret that these fragments belong to a single individual, the individual D. The shaft is robust but laterally compressed. Both rami diverge with an angle of nearly 35°–40°. The haemal canal is apparently deep (Figure 7(c)). According to the classification of Otero et al. (2011), the chevrons are 'straight open-shaped', which suggests that these fragments pertain to the anterior part of the tail.

3.3 Appendicular skeleton

3.3.1 Forelimb

Humerus. There is a left humerus that corresponds to a small specimen; it is assigned to the specimen D (originally, it was included as part of the holotype by Martinelli and Forasiepi 2004) (Figure 8). This is a gracile bone, with a narrow and rather straight shaft. Both the proximal and distal ends are expanded, being the width of the proximal end nearly twice that of the diaphysis (retention index, RI: 0.277). The RI matches approximately with the value obtained in *L. astibiae* (Díez Díaz et al. 2013b). The medial border is slightly more concave than the lateral one, as common among titanosaurs. The proximal border is arched and the distal border is straight. The general proportions resemble those of several non-saltasaurine titanosaurs, such as *Epachthosaurus* (Martinez et al. 2004), *Mendozasaurus* and *Rapetosaurus*, differing from the short and stout bone observed in *Neuquensaurus* and *Saltasaurus*, as Martinelli and Forasiepi (2004) recognise.

The humeral head is rounded, well developed and medially oriented. Although partially eroded, the deltopectoral crest extends until the mid-length of the bone (Figure 8(b)). The anterior face of the proximal humerus is slightly convex, whereas the distal half is flat. Conversely, the posterior face of the proximal half of the bone is markedly concave. Distally, a triangular and convex anconeal fossa is developed.

As in *Bonitasaura salgadoi*, the lateral and medial condyles have the same distal extension, unlike *Epachthosaurus* and *Rapetosaurus* where the lateral condyle is more developed.

Metacarpal I. There are two metacarpals I (Figure 9(a),(d)). One, left, may belong to the individual A (Figure 9(a)); the other, right and smaller, probably belongs to the individual E (Figure 9(d)). The largest element (numbered as MACN-PV RN 821 but included by Martinelli and Forasiepi (2004) in the specimen MACN-PV RN 1061) was erroneously described by Martinelli and Forasiepi (2004, p. 282) as a left radius, and the smallest element was neither described nor figured.

The metacarpal I of individual A is straight, as in *Epachthosaurus* and *Rapetosaurus*, differing from the bowed metacarpal I of *Antarctosaurus* (Huene 1929) and *Argyrosaurus* (Mannion and Otero 2012). It is long and slender, with proximal and distal ends slightly expanded (RI: 0.237) (Figure 9(a)), as in *Rapetosaurus*. Its proximal portion is damaged, but it seems to be lateromedially compressed. Its mid-shaft is oval in cross section, with nearly flat lateral and medial surfaces. The proximal contact with the metacarpal II cannot be observed; however, the distal contact is evident, with a short concave surface pointing anteromedially. The distal end is subtriangular.

The metacarpal I of the individual E (Figure 9(d)) is proportionally shorter, and has its proximal and distal ends more expanded than the individual A (RI: 0.28). Its proximal end is subrectangular, and it has a rugose surface. On the other hand, its distal end is suboval and it is 30° twisted respect to the proximal end.

Metacarpal IV. The right metacarpal IV, here assigned to the individual A, was erroneously described as a left ulna by Martinelli and Forasiepi (2004, Fig. 18B) (Figure 9(b)). It is complete, well preserved and slightly shorter than the metacarpal I. The epiphyses are expanded, mostly the proximal one (RI: 0.32). The proximal end is subtriangular in proximal view and its surface rugose; the anterior border is concave and the posteromedial border flat. On the anterior aspect, a wide and concave triangular zone is developed along the proximal mid-length; this represents the contact surface with the metacarpal III.

On the posterior face of the distal half, there is a well-developed ridge. In medial view, this structure forms a conspicuous step on the posterior border before reaching the distal contact with the metacarpal V (Figure 9(b), 'pr'), unlike *Rapetosaurus* and *Epachthosaurus*, where the ridge is absent. Like the proximal contact with the metacarpal III, the contact with the metacarpal V is triangular and well developed. However, it is nearly flat and located on the posterior aspect of the bone. The distal end is sub-trapezoidal and rugose.

Metacarpal V. A small right metacarpal V is assigned to the individual E (Figure 9(c)). This bone was neither described nor figured by Martinelli and Forasiepi (2004). As the metacarpal I of the same individual, this element is proportionally short and transversally expanded (RI: 0.322), more than that of *Rapetosaurus* and *Epachthosaurus.*

The proximal end is subtriangular, with a broad anterior side. The anterior face is rather flat, so that the contact surface with the metacarpal IV cannot be recognised. On the other hand, the posterior side of the metacarpal V is slightly convex on its proximal mid-length, becoming strongly convex distally. The distal end is sub-quadrangular and rugose, and twists 40° respect to the proximal end.

3.3.2 Hindlimb

Femur. Both femora are assigned to the individual B (the right one is incomplete) (Figure 10(a),(b)), and a third right femur is assigned to the individual D (Figure 10(c)). Although the femora assigned to both individuals are slender and proportionally similar (individual B, RI: 0.231; individual D, RI: 0.23), they show minor morphological differences. The RI is higher than that observed in *L. astibiae* (Díez Díaz et al. 2013b). The femur of the individual B has a globose femoral head, dorsomedially exposed, but with a strong medial projection (Figure 10(a),(b)), as in *Rapetosaurus* and *Neuquensaurus*. Conversely, the individual D (Figure 10(c)) does not present this condition. The individual B has a greater trochanter in a nearly straight angle with respect to the lateral border, as in *Magyarosaurus* (FGGUB-1511) differing from the obtuse angle observed in the individual D and in most titanosaurs, such as *Epachthosaurus*, *Rapetosaurus*, *Rocasaurus* and *Neuquensaurus.* A short lateral bulge, proximally located, is observed in the individual B, as occurs in *Magyarosaurus*. On the other hand, the lateral bulge of the individual D extends until the mid-shaft of the femur. The *femorotibialis crest* is evident only in the anterior face of the individual D (Figure 10(c)); however, the trochanteric shelf can be recognised in the individual B (Figure 10(a)). The medial border of the femur of the individual B is straight, practically throughout its entire length, unlike the curved medial border that is present in the individual D. Only the distal end of the individual B is complete. Both condyles have a similar anteroposterior extension, as in *Magyarosaurus*, and differ from the condition observed in *Rapetosaurus* and *Bonitasaura,* in which the tibial condyle is more expanded. Moreover, the fibular condyle has a greater transverse development, as in *Rapetosaurus* and *Neuquensaurus*. Remarkably, the tibial condyle is not medially projected as seen in most titanosaurs. Whatever this condition, both condyles are anteriorly exposed, as in *Lirainosaurus*,

Rinconsaurus (Calvo and González Riga 2003), *Rapetosaurus*, *Neuquensaurus* and *Saltasaurus*.

Although individuals B and D have femora of similar RI, some differences in these bones suggest the presence of two 'morphs' (as occurs with the materials assigned to both *Neuquensaurus* and *Saltasaurus*); however, at present we cannot know whether they represent two different species or different sexes.

Tibia. The three tibiae collected are assigned to the individuals A (Figure 11(a)), B (Figure 11(b)) and D (Figure 11(c)). The tibia of the individual A lacks its distal end; those of the individuals B and D are almost complete. As occurs with the femora, the tibiae of the individuals A and B (similar in size and morphology) differ from that of the smaller individual D, although both are slender (individual B, RI: 0.266; individual D, RI: 0.257), with RI values higher than those observed in *Lirainosaurus* (Díez Díaz et al. 2013b). The anteroposterior proximal width of the tibiae of both individuals doubles its distal width; nonetheless, the proximal end of the tibia of the individual B is lateromedially wider. The proximal surface of the tibia of the individual B is subtriangular (Figure 11(b)), differing from the ovoidal perimeter present in the individual D (Figure 11(c)).

In lateral view, the cnemial crest of the tibia of the individual B is reduced and restricted to the proximal quarter of the bone, and it has a curved border. Conversely, in the individual D, as in most titanosaurs (e.g. *Epachthosaurus*, *Mendozasaurus*, *Rapetosaurus*, *Bonitasaura*, *Laplatasaurus* (Powell 2003) and *Neuquensaurus*), the cnemial crest is more expanded, with a triangular border and a well-developed, shallow groove. The tibia of the individual B has a curved anterior border, and a nearly straight posterior border, as in many titanosaurs, such as *Epachthosaurus*, *Rapetosaurus*, *Bonitasaura* and *Neuquensaurus*. On the contrary, the proximal third of the tibia of the individual D is posteriorly oriented, describing a curved posterior border.

The distal ends of the tibiae of both individuals also differ; in the individual B, it is more rounded than that of the individual D, which is angulate. Furthermore, the latter presents a more twisted distal end. In the individual B, the lateral condyle is smaller and located above the level of the posterior condyle. The condyles of the individual D are similar in size.

Fibula. The left fibula (Figure 12(a)), here assigned to the individual B, is extremely narrow (RI: 0.149), noticeably similar to that of *Malawisaurus* (Gomani 2005), *Rapetosaurus* and *Lirainosaurus*. Both epiphyses of this bone are expanded, specially the proximal end. This latter has a drop-shaped cross section, with a narrow anterior projection. On the contrary, the distal end is subtriangular in distal view.

The fibula is nearly straight along its entire length, except for a slight curvature of its proximal quarter, only observed in anterior view. The lateral surface of the bone is convex, and the medial surface, which contacts the tibia, nearly flat. The lateral trochanter is much more pronounced than in *Rapetosaurus* and located more proximally on its lateral aspect. It is a simple longitudinal bump, differing from the double lateral structure, although variable in morphology, present in *Epachthosaurus*, *Antarctosaurus*, *Laplatasaurus* and *Uberabatitan*. A slightly concave triangular surface, distally located on the medial aspect, contacts the lateral condyle of the tibia.

Astragalus. There are two astragali, none of which were described nor figured by Martinelli and Forasiepi (2004); one left, nearly complete, is assigned to the individual D (Figure 12(c)), the other, right and incomplete, to the individual B (Figure 12(b)). Both elements are similar in their general morphology. Thus, the description given below is focused on the individual D.

In anterior view, the astragalus is triangular in shape. The dorsal (tibial contact) and lateral (fibular contact) surfaces are flat. On the other hand, the ventral margin is curved. The surface of the astragalus is mostly rugose. The ascending process is low and rounded (Figure 12(c)). Unlike other titanosaurs, such as *Bonitasaura*, *Opisthocoelicaudia* (Borsuk-Bialynicka 1977) and *Neuquensaurus*, a medial deep foramen is not recognised in the individual D. However, in the astragalus of the individual B, a partially developed foramen seems to be present on the medial aspect.

Metatarsal I. A nearly complete left metatarsal I is assigned to the individual A (Figure 13(a)), and a fragmentary metatarsal I to the individual D (Figure 13 (d)). The metatarsal I of *Bonatitan* is short and robust, although a bit slender than the corresponding bone in *Epachthosaurus*, *Rapetosaurus* and *Bonitasaura*. Its proximal and distal ends are anteroposteriorly and lateromedially expanded, respectively. The proximal end is subquadrangular, although the laterodorsal border is eroded. The dorsal face of this metatarsal is nearly flat, and the ventral face is concave. On the lateral surface, a triangular and flat proximal zone represents the contact with the metatarsal II. This area is ventrally bounded by an oblique ridge. The distal end is rugose and markedly convex, with an ovoid perimeter that is slightly constricted in the mid-width.

Metatarsal III. A proximal fragment of a metatarsal III, probably belonging to the individual A (Figure 13(b)), and a distal fragment of another, presumably of the individual D (Figure 13(e)), are preserved. In addition, a complete left? metatarsal III? is tentatively assigned to the individual D (Figure 13(h)), although it could belong to a smaller individual.

Both proximal and distal ends are expanded, although the proximal end is the widest. This end is sub-rhomboidal in the individual A (Figure 13(b)) and subtriangular in the individual D (Figure 13(h)). The dorsal surface is slightly

convex, while the ventral surface is flat. The distal end, convex and rugose, is sub-quadrangular in the individual B (Figure 13(b)) and more rounded in the individual D (Figure 13(h)).

Metatarsal V. A proximal fragment of a metatarsal V is assigned to the individual A (Figure 13(c)), while both proximal and distal halves of metatarsal V are assigned to the individual D (Figure 13(f),(g)).

As in other titanosaurs, this bone is characterised by its proximal expansion, fan-shaped and distal reduction. In addition, a strong lateral compression is typical in this metatarsal. The proximal end is ovoid and elongated; its medial face, which contacts the metatarsal IV, is flat (Figure 13(f)). The lateral surface is somewhat convex. The distal end is ovoidal in shape and it has a convex surface (Figure 13(g)).

Phalanx. An ungual phalanx is assigned to the individual D (Figure 13(i)). Compared with complete titanosaurian pedes (e.g. *Epachthosaurus*, *Opisthocoelicaudia*, titanosaur from 'La Invernada' site, Neuquén, MUCPv-1533, González Riga et al. 2008), it presumably belongs to the digit II or III.

The proximal end of the phalanx is ovoid and nearly flat, devoid of a dorsal intercondylar process. Although slightly curved, it is sickle-shaped in lateral view. The surface is dominated by minuscule furrows and small isolated foramina. On the ventral margin, a well-marked longitudinal process develops along the distal mid-length of the phalanx as in *Mendozasaurus*, *Rapetosaurus* and MUCPv-1533.

4. Phylogenetic analysis

The original claim that *B. reigi* is a member of the Saltasaurinae (Martinelli and Forasiepi 2004) was corroborated in the cladistic analysis carried out by Filippi et al. (2011), in fact, the only one that included that species. Using the data matrix of Calvo et al. (2007), they conclude that *Bonatitan* was a saltasaurine 'based on the following characters: anterodorsal border of the neural spine in middle caudal vertebrae, posterior located on regarding the anterior border of the postzygapophyses (37.1), and distal condyle of the femur anteriorly expanded (64.1)' (Filippi et al. 2011, p. 518). However, there are some problems with this hypothesis: first, the numbers of characters cited (37 and 64) from the character list of Calvo et al. (2007) are incongruent with their description; second, the character 'distal condyle of the femur anteriorly expanded' is not present in the data matrix of Calvo et al. (2007); third, running the matrix of Filippi et al. (2011), in fact five synapomorphies (characters 14, 19, 20, 35 and 40) support *Bonatitan* within Saltasaurinae (Filippi personal communication), but only the last one ('anterodorsal border of the neural spine in middle caudal vertebrae, posterior located on regarding the anterior border of the postzygapophyses') can be corroborated in the specimen, and was erroneously coded, as mentioned above.

In order to test the relationships of *B. reigi* within Titanosauria, a phylogenetic analysis was performed using TNT v. 1.1 (Goloboff et al. 2000) with a data matrix of 77 characters and 22 taxa (Appendix). The matrix was based in that of Gallina and Apesteguía (2011), with minimal modifications. Two characters were added: 74, femoral distal condyles, articular surface shape: restricted to distal portion of femur (0); expanded onto anterior portion of femoral shaft (1) (Wilson 2002); and 76, Tibial robustness: gracile, RI $\leq$ 0.3 (0); robust, RI $>$ 0.3 (1). The terminal taxa include those of Gallina and Apesteguía (2011), except for the exclusion of *Antarctosaurus wichmanianus* (Huene 1929), which presents problems in the recognition of type materials (Gallina in preparation), and the addition of *B. reigi* (Martinelli and Forasiepi 2004). *Camarasaurus* was used as outgroup and multistate characters were

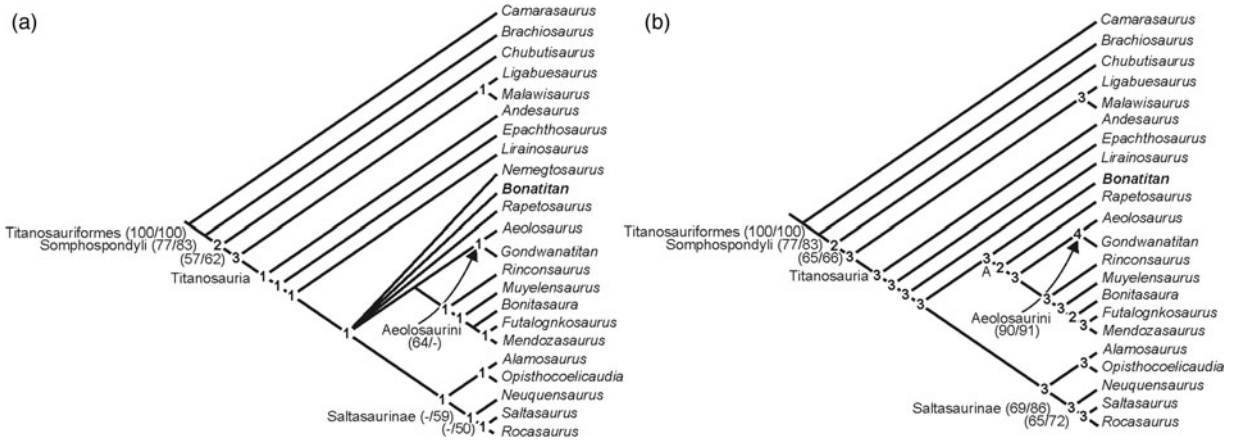

Figure 14. Phylogenetic relationships of *B. reigi*. (a) Strict consensus tree of three most parsimonious trees (CI: 0.66, ReI: 0.71). (b) Reduced consensus tree excluding *Nemegtosaurus*. Bootstrap and Jackknife values up to 50% indicated in brackets.

treated as unordered. The search, performed using 1000 replicates of Wagner trees, found three equally most parsimonious trees with relatively high indices (141 steps, consistency index (CI): 0.66, retention index (ReI): 0.71). The best score was obtained in 99% of the replicates. The strict consensus tree collapsed into a polytomy at the base of Titanosauria, although preserved well-supported groups such as Aeolosaurini and Saltasaurinae (Figure 14(a)). In this tree, *B. reigi* is recovered in a basal position in the polytomy not related to the Saltasaurinae. Besides, a constrained search showed that two additional steps are required to place *Bonatitan* within Saltasauridae.

With the aim of examining the polytomy at the base of Titanosauria, individual taxa were removed for the consensus and reincluded one at a time for the final analysis. The exclusion of *Nemegtosaurus* resolved the polytomy (Figure 14(b)), substantially improved the support of most nodes as Aeolosaurini and Saltasaurinae, and recovered *B. reigi* as the sister taxon of (*Rapetosaurus* + (Aeolosaurini + (*Rinconsaurus* + (*Muyelensaurus* + (*Bonitasaura* + (*Futalognkosaurus* + *Mendozasaurus*))))))) in node A. This node is supported by three characters: (2.1), (12.1) and (32.2).

5. Conclusion

The material assigned to *B. reigi* (Martinelli y Forasiepi 2004) is reorganised in five individuals as well as redescribed. The braincase MACN-PV RN 821, probably pertaining to the individual C, is designated as the only element of the holotype, and the rest of the material labelled as specimen MACN-PV RN 821 as part of the referred material. Several undescribed materials from the appendicular and axial skeleton are described for the first time: sacral ribs, haemal arches, metatarsals, metacarpals and astragali.

B. reigi is rediagnosed on the basis of a combination of characters, most of which are those of the original diagnosis. Two new characters are incorporated into the emended diagnosis: small paired pits on the frontals and posterior ridge of the metacarpal IV. The other characters of the diagnosis are left, with the only exception of longitudinal groove located on the suture between the parietals that continues posteriorly over the supraoccipital to the foramen magnum.

In our phylogenetic analysis, *Bonatitan* is recovered within Titanosauria as a basal member of a wide clade recovered as the sister group of the Saltasauridae. Its inclusion within the Saltasaurinae (postulated by Martinelli and Forasiepi 2004) is not corroborated in our analysis.

Acknowledgements

The authors thank Alejandro Kramarz and Stella Maris Álvarez (MACN), for allowing us the access to materials under their care, and Alejandro Otero for the critical review of the manuscript.

Notes

1. Email: pablogallina@gmail.com
2. Email: a.paulinacarabajal@conicet.gov.ar

References

Bonaparte JF, Coria RA. 1993. Un nuevo y gigantesco saurópodo titanosaurio de la Formación Río Limay (Albiano–Cenomaniano) de la Provincia del Neuquén. Argentina. Ameghiniana. 30:271–282.

Bonaparte JF, González Riga BJ, Apesteguía S. 2006. *Ligabuesaurus leanzai* gen. et sp. nov. (Dinosauria, Sauropoda), a new titanosaur from the Lohan Cura Formation (Aptian, Lower Cretaceous) of Neuquén, Patagonia, Argentina. Cretaceous Res. 27:364–376.

Borsuk-Bialynicka M. 1977. A new camarasaurid sauropod *Opisthocoelicaudia skarzynskii*, gen. n. sp. n. from the Upper Cretaceous of Mongolia. Palaeontol Pol. 37:45–64.

Calvo JO, González Riga BJ. 2003. *Rinconsaurus caudamirus* gen. et sp. nov., a new titanosaurid (Dinosauria, Sauropoda) from the Late Cretaceous of Patagonia, Argentina. Rev Geol Chile. 30 (2):333–353.

Calvo JO, Kellner AW. 2006. Description of a sauropod dinosaur braincase (Titanosauridae) from the Late Cretaceous Río Colorado Subgroup, Patagonia. An Acad Bras Ciênc. 78:175–182.

Calvo JO, Salgado L. 1995. *Rebbachisaurus tessonei* sp. nov. A new Sauropoda from the Albian-Cenomanian of Argentina; new evidence on the origin of the Diplodocidae. Gaia. 11:13–33.

Calvo JO, Porfiri JD, González Riga BJ, Kellner AWA. 2007. A new Cretaceous terrestrial ecosystem from Gondwana with the description of a new sauropod dinosaur. An Acad Bras Ciênc. 79(3):529–541.

Campos D, Kellner AWA, Bertini RJ, Santucci RM. 2005. On a titanosaurid (Dinosauria, Sauropoda) vertebral column from the Bauru Group, Late Cretaceous of Brazil. Arq Mus Nac Rio J. 63(3):565–593.

Curry Rogers K. 2005. Titanosauria: a phylogenetic overview. In: Curry Rogers K, Wilson JA, editors. The sauropods: evolution and paleobiology. Berkeley: University of California Press; p. 50–103.

Curry Rogers KA. 2009. The postcranial osteology of *Rapetosaurus krausei* (Sauropoda: Titanosauria) from the Late Cretaceous of Madagascar. J Vert Paleontol. 29(4):1046–1086.

Curry Rogers KA, Forster CA. 2001. The last of the dinosaur titans: a new sauropod from Madagascar. Nature. 412:530–534.

Curry Rogers KA, Forster CA. 2004. The skull of *Rapetosaurus krausei* (Sauropoda: Titanosauria) from the Late Cretaceous of Madagascar. J Vert Paleontol. 24:121–144.

Díez Díaz V, Pereda Suberbiola X, Sanz JL. 2011. Braincase anatomy of the sauropod dinosaur *Lirainosaurus astibiae* (Titanosauria) from the Late Cretaceous of the Iberian Peninsula. Acta Paleontol Pol. 56:521–533.

Díez Díaz V, Pereda Suberbiola X, Sanz JL. 2013a. The axial skeleton of the titanosaur *Lirainosaurus astibiae* (Dinosauria: Sauropoda) from the latest Cretaceous of Spain. Cretaceous Res. 43:145–160.

Díez Díaz V, Pereda Suberbiola X, Sanz JL. 2013b. Appendicular skeleton and dermal armour of the Late Cretaceous titanosaur *Lirainosaurus astibiae* (Dinosauria: Sauropoda) from Spain. Palaeontol Electron. 16(2): 19A, 18p.

Filippi LS, García RA, Garrido CA. 2011. A new titanosaur sauropod dinosaur from the Upper Cretaceous of North Patagonia, Argentina. Acta Palaeontol Pol. 56(3):505–520.

Filippi LS, Garrido CA. 2008. *Pitekunsaurus macayai* gen. et sp. nov., nuevo titanosaurio (Saurischia, Sauropoda) del Cretácico Superior de la Cuenca Neuquina, Argentina. Ameghiniana. 45:575–590.

Franco-Rosas AC, Salgado L, Rosas CF, Carvalho IS. 2004. Nuevos materiales de titanosaurios (Sauropoda) en el Cretácico Superior de Mato Grosso. Revista Brasileira de Paleontologia. 7(3):329–336.
Gallina PA, Apesteguía S. 2011. Cranial anatomy and phylogenetic position of the titanosaurian sauropod *Bonitasaura salgadoi*. Acta Palaeontol Pol. 56:45–60.
García RA, Paulina Carabajal A, Salgado L. 2008. Un nuevo basicráneo de titanosaurio de la Formación Allen (Campaniano Maastrichtiano), Provincia de Río Negro, Patagonia, Argentina. Geobios. 41:625–633.
Gauthier JA. 1986. Saurischian monophyly and the origin of birds. In: Padian K, editor. The origin of Birds and the evolution of Flight. Berkeley: Memoirs of the California Academy of Sciences 8; p. 1–55.
Goloboff PA, Farris JS, Nixon KC. 2000. T.N.T. "Tree Analysis Using New Technology". Tucumán: Published by the authors. Available at www.cladistics.org
Gomani EM. 2005. Sauropod dinosaurs from the Early Cretaceous of Malawi, Africa. Palaeontol Electron. 8(1.27A):1–37.
González Riga BJ. 2003. A new titanosaur (Dinosauria, Sauropoda) from the Upper Cretaceous of Mendoza Province, Argentina. Ameghiniana. 40(2):155–172.
González Riga BJ. 2005. Nuevos restos fósiles de *Mendozasaurus neguyelap* (Sauropoda: Titanosauridae) del Cretácico Tardío de Mendoza, Argentina. Ameghiniana. 42(3):535–538.
González Riga BJ, Calvo JO, Porfiri J. 2008. An articulated titanosaur from Patagonia (Argentina): new evidence of neosauropod pedal evolution. Paleoworld. 17:33–40.
Huene F. 1929. Los Saurisquios y Ornitisquios del Cretáceo Argentino. An Mus Plata. 2:1–196.
Kurzanov SM, Bannikov AF. 1983. A new sauropod from the Upper Cretaceous of Mongolia. Palaeontol J. 2:91–97.
Lehman TM, Coulson AB. 2002. A juvenile specimen of the sauropod dinosaur *Alamosaurus sanjuanensis* from the Upper Cretaceous of BigBend National Park, Texas. J Paleontol. 76:156–172.
Mannion PD, Otero A. 2012. A reappraisal of the Late Cretaceous Argentinean sauropod dinosaur *Argyrosaurus superbus*, with a description of a new titanosaur genus. J Vert Paleontol. 32(3):614–638.
Marsh OC. 1878. Principal characters of American Jurassic dinosaurs. Part I. Am J Sci. 16:411–416.
Martinelli AG, Forasiepi A. 2004. Late Cretaceous vertebrates from Bajo de Santa Rosa (Allen Formation), Río Negro province, Argentina, with the description of a new sauropod dinosaur (Titanosauridae). Rev Mus Argent Cienc Nat. 6:257–305.
Martínez RD, Giménez O, Rodríguez J, Luna M, Lamanna MC. 2004. An articulated specimen of the basal titanosaurian (Dinosauria: Sauropoda) *Epachthosaurus sciuttoi* from the Early Late Cretaceous Bajo Barreal Formation of Chubut Province, Argentina. J Vert Paleontol. 24(1):107–120.
McIntosh JS. 1990. Sauropoda. In: Weishampel DB, Dodson P, Osmólska H, editors. The Dinosauria. Berkeley: University of California Press; p. 345–390.
Novas FE, Pol D, Canale JI, Porfiri JD, Calvo JO. 2008. A bizarre Cretaceous theropod dinosaur from Patagonia and the evolution of Gondwanan dromaeosaurids. Proc R Soc B., doi:10.1098/rspb.2008.1554.
Otero A, Gallina PA, Canale JI, Haluza A. 2011. Sauropod haemal arches: morphotypes, new classification and phylogenetic aspects. Hist Biol. 24(3):243–256.
Owen R. 1842. Report on British fossil reptiles, Part II. Rep Brit Assoc Adv Sci. 11:60–204.
Paulina Carabajal A. 2012. Neuroanatomy of titanosaurid dinosaurs from the Upper Cretaceous of Patagonia, with comments on endocranial variability within Sauropoda. Anat Rec. doi:10.1002/ar.22572.
Paulina Carabajal A, Salgado L. 2007. El basicráneo de un titanosaurio (Dinosauria, Sauropoda) del Cretácico Superior del norte de Patagonia: descripción y aportes al conocimiento del oído interno de los dinosaurios. Ameghiniana. 44:109–120.
Powell JE. 1986. Revisión de los Titanosáuridos de América del Sur. Tucumán [PhD thesis]. Tucumán, Argentina: Universidad Nacional de Tucumán. 340pp.
Powell JE. 2003. Revision of South American titanosaurid dinosaurs: paleobiological, palaeobiogeographical and phylogenetic aspects. Rec Queen Victoria Museum Launceston. 11:1–173.
Salgado L, Azpilicueta C. 2000. Un nuevo saltasaurino (Sauropoda, Titanosauridae) de la provincia de Río Negro (Formación Allen, Cretácico Superior), Patagonia, Argentina. Ameghiniana. 37:259–264.
Salgado L, Calvo JO. 1997. Evolution of titanosaurid sauropods. II: the cranial evidence. Ameghiniana. 34:33–48.
Salgado L, Carvalho IS. 2008. *Uberabatitan ribeiroi*, a new titanosaur from the Marilia Formation (Bauru group, Upper Cretaceous); Minas Gerais, Brazil. Palaeontology. 51(4):881–901.
Salgado L, Apesteguía S, Heredia SE. 2005. A new specimen of *Neuquensaurus australis*, a Late Cretaceous saltasaurine titanosaur from North Patagonia. J Vert Paleontol. 25(3):623–634.
Salgado L, Coria RA, Calvo JO. 1997. Evolution of titanosaurid sauropods I: Phylogenetic analysis based on the postcranial evidence. Ameghiniana. 34(1):3–32.
Salgado L, Coria RA, Magalhaes Ribeiro CM, Garrido AC, Rogers R, Simón ME, Arcucci AB, Curry Rogers KA, Paulina Carabajal A, Apesteguía S, et al. 2007. Upper Cretaceous dinosaur nesting sites of Río Negro (Salitral Ojo de Agua and Salinas de Trapalcó-Salitral de Santa Rosa), Northern Patagonia, Argentina. Cretaceous Res. 28(3):392–404.
Salgado L, Powell JE. 2010. Reassessment of the vertebral laminae in some South American titanosaurian sauropods. J Vert Paleontol. 30:1760–1772.
Upchurch P. 1998. The phylogenetic relationships of sauropod dinosaurs. Zoological Journal of the Linnean Society. 124:43–103.
Wilson JA. 2002. Sauropod dinosaur phylogeny: critique and cladistic analysis. Zool J Linn Soc. 136:217–276.
Wilson JA. 2005. Redescripction of the Mongolian Sauropod *Nemegtosaurus mongoliensis* Nowinski (Dinosauria: Saurischia) and comment son Late Cretaceous Sauropod Diversity. J Syst Palaeontol. 3(3):283–318.
Wilson JA. 2011. Anatomical terminology for the sacrum of sauropod dinosaurs. Contrib Mus Paleontol Univ Michigan. 32:59–69.
Wilson JA, D'Emic MD, Curry Rogers KA, Mohabey DM, Sen S. 2009. Reassessment of the sauropod dinosaur *Jainosaurus (="Antarctosaurus") septentrionalis* from the Upper Cretaceous of India. Contrib Mus Paleontol Univ Michigan. 32(2):17–40.
Wilson JA, D'Emic MD, Ikejiri T, Moacdieh EM, Whitlock JA. 2011. A nomenclature for vertebral fossae in sauropods and other saurischian dinosaurs. PloS ONE. 6(2), doi:10.1371/journal.pone.0017114.
Wilson JA, Sereno PC. 1998. Early evolution and higher-level phylogeny of sauropod dinosaurs. J Vert Paleontol. 18(supplement 2 (Society of Vertebrate Paleontology, Memoir 5)):1–68.

Appendix

Data matrix

Camarasaurus	0010001100	1000000000	0000000000	0000000000	0000000000	0000000000	0000000000	0000000
Brachiosaurus	0000011000	0000010101	1000010010	1000100000	0000000010	0000000000	0000000010	111000?
Chubutisaurus	??????????	??????????	??????????	????2?0001	?0??00001?	????0???00	????0?????	?11010?
Ligabuesaurus	??????????	???????1?1	?00101010?	1110111111	??????????	???????10?	????0?????	?110100
Malawisaurus	0???11??0?	????000201	?1000?00??	11?0111111	??10002010	0?11010???	1110??10??	????10?
Andesaurus	??????????	??????????	??????????	1??0111011	?0?0001010	0010000?0?	????1110??	?01????
Epachthosaurus	??????????	??????????	??????????	1011211011	11?0002210	0011000101	11??11??11	101?101
Lirainosaurus	??????????	?????0?2?1	??????????	10?1211111	?11?002210	0000000?01	?101??????	??11?0?
Nemegtosaurus	101111010?	1110110221	??????????	??????????	??????????	??????????	??????????	???????
Bonatitan	?111111??	?11100????	?0????????	121?2??111	??1?0?2?10	020?010?01	????1?????	?01110?
Rapetosaurus	1111110111	1111110221	2000010?1	1211211111	1?00002210	010?000101	110??11011	1011?01
Aeolosaurus	??????????	???????221	??????????	1???2?????	?30?012220	1102001?01	?10?1101??	??1?1??
Gondwanatitan	??????????	??????????	??????????	1?11211111	11???12220	1002001?0?	??????0111	????1??
Rinconsaurus	??????????	???????211	?00001011?	1011211111	1???002210	0111011101	1101111111	101??0?
Muyelensaurus	?1?1??11??	?1?111?211	?1000?011?	1211211111	1?0?002210	0211011101	110?111111	101?1??
Bonitasaura	?11111?1?1	??????1211	???101121?	1201211111	?110002210	0101011?01	?1??1112??	?011100
Futalognkosaurus	??????????	??????????	2101011222	1?0?2??111	111?0?2?1?	?1??0?????	?????11211	1??????
Mendozasaurus	??????????	??????????	??010?122?	120?2??111	?110002110	0111000101	111?1?????	?01?101
Alamosaurus	??????????	???????22?	?00001001?	1??1200111	1311002210	0200000101	1111111211	101?1??
Opisthocoelicaudia	??????????	??????????	?????????1	0011210111	1211000010	0200000111	1101111111	1010101
Neuquensaurus	??????????	??????????	?010010012?	1011211111	131?102211	0200000101	11011?1211	1?1111?
Saltasaurus	?01??111??	?01111?221	?010110012?	1111211111	110?102211	0200100112	1101111211	101111?
Rocasaurus	??????????	??????????	??????01??	1011211111	????102211	0?00100???	?????11211	1?1????

Character list

1. Short deep snout: present (0); absent (1) (modified from Upchurch 1998 by Curry Rogers 2005).
2. Frontal contribution to supratemporal fossa: absent (0); present (1) (Wilson and Sereno 1998).
3. Frontal, dorsal texture: smooth (0); rugose (1) (Gallina and Apesteguía 2011).
4. Parietal–occipital process, dorsoventral height: deep, nearly twice the diameter of the foramen magnum (0); short, less than the diameter of the foramen magnum (1) (Wilson 2002).
5. Parietal, elongate lateral process: absent (0); present (1) (Curry Rogers 2005).
6. Parietal, cranial inclination with wide caudodorsal exposure of crest: absent (0); present (1) (Salgado et al. 1997).
7. Parietal, contribution to post-temporal fenestra: absent (0); present (1) (Wilson 2002).
8. Parietal, distance separating supratemporal fenestrae: less than (0); or twice (1); the long axis of supratemporal fenestra (Wilson 2002).
9. Ascending process of premaxilia: directed dorsally (0); directed caudodorsally (1) (Gauthier 1986).
10. External nares, configuration of lateral margin: lacrimal excluded, maxilla–nasal contact (0); lacrimal participates, separates maxilla and nasal (1) (Gallina and Apesteguía 2011).
11. Preantorbital fenestra: absent (0); present (1) (Wilson and Sereno 1998).
12. Supraoccipital, height: twice (0); subequal (1); or less (2) than height of foramen magnum (Wilson 2002).
13. Paroccipital process, ventral non-articular process: absent (0); present (1) (Wilson 2002).
14. Longitudinal groove on the supraoccipital: absent (0); present (1) (Curry Rogers 2005).
15. Basipterygoid processes, angle of divergence: approximately 45° (0); less than 30° (1); over 45° (2) (Wilson 2002).
16. Basal tubera, craniocaudal depth: approximately half dorsoventral height (0); sheetlike 20% dorsoventral height (1) (Wilson 2002).
17. Mandible shape: U shape (0); L shape (1) (Gallina and Apesteguía 2011).
18. Tooth shape: spoon-like (0); compressed cone chisel-like (1); pencil chisel-like (2) (Calvo and González Riga 2003).
19. Tooth crowns, cross-sectional shape at mid-crown: D-shaped (0); subcylindrical with smooth crest (1); cylindrical (2) (modified from Wilson and Sereno 1998).
20. Wear facets of teeth sharply inclined: absent (0); present (1) (Salgado and Calvo 1997).
21. Cervical vertebrae, number: 12 (0); 13 (1); 14 or more (2) (Upchurch 1998).
22. Pleurocoels in anterior and middle cervical vertebrae: present (0); absent (1) (modified from Calvo and Salgado 1995).
23. Cervical prezygapophyses, relative length: articular facets that surpass (0), or not surpass (1) the centra (Salgado et al. 1997).
24. Posterior cervical neural spines laterally expanded and wider than the centra: absent (0); present (1) (González Riga 2005).
25. Neural spines in cervical vertebrae: tall (0); small (1) (modified from Calvo and Salgado 1995).
26. Anterior cervical neural spines: bifid (0); single (1) (Upchurch 1998).
27. Posterior cervical vertebrae, proportions: ratio of total height/centrum length: less (0), or more (1) than 1.5 (modified from Calvo and Salgado 1995 by González Riga 2005).
28. Supradiapophyseal fossa in posterior cervical vertebrae: absent (0); shallow or reduced (1); deep and extended (2) (González Riga 2005).
29. Posterior cervical centra, proportions: ratio of anteroposterior length/height of posterior face: >3 (0); between 2.5 and 1.5 (1); <1.5 (2) (modified from Wilson 2002).
30. Dorsal vertebrae, number: 12 (0); 11 (1); 10 or fewer (2) (Wilson and Sereno 1998).
31. Anterior dorsal neural spines, shape: bifid (0); single (1) (McIntosh 1990).
32. Anterior dorsal vertebrae, infrapostzygapophyseal fossa: absent (0); present not divided (1); present divided into two subtriangular fossa (2) (Gallina and Apesteguía 2011).
33. Anterior dorsal neural spines inclined posteriorly more than 20° from vertical: absent (0); present (1) (modified from Wilson and Sereno 1998).
34. Posterior dorsal neural spines, dorsal development: more (0), or less (1) than 20% of the total height of the vertebra (González Riga 2003).
35. Prespinal lamina in dorsal vertebrae: absent (0); present in the distal end of neural spine (1); present all along the neural spine (2) (Salgado et al. 1997).
36. Centroparapophyseal lamina in posterior dorsal vertebrae: absent (0); present (1) Bonaparte and Coria 1993).
37. Ventrally widened or slightly forked centrodiapophyseal laminae in posterior dorsal vertebrae: absent (0); present (1) (Salgado et al. 1997).
38. Hyposphene–hypantrum articulation in dorsal vertebrae: present (0); absent (1) (Salgado et al. 1997).
39. Pleurocoels in dorsal vertebrae shape: circular or elliptical (0); posteriorly acuminate (1) (Salgado et al. 1997).
40. Camellate or somphospondylous types of internal structures of presacral vertebrae: absent (0); present (1) (modified from Wilson and Sereno 1998 by González Riga 2003).
41. Sacral vertebrae, number: five (0); six or more (1) (McIntosh 1990).
42. First caudal vertebrae, type: platycoelous (0); procoelous (1); opisthocoelous (2); biconvex (3) (Salgado et al. 1997).
43. Wide and deep interzygapophyseal cavity in caudal vertebrae: absent (0); present (1) (Calvo et al. 2007).
44. Caudal transverse processes: disappear by caudal 15 (0); disappear by caudal 10 (1) (Wilson 2002).
45. Anterior and middle caudal centra, proportions: as high as wide (0); depressed, wider than high (1) (Salgado et al. 1997).
46. Mid caudal centra with the anterior face strongly inclined anteriorly: absent (0); present (1) (Franco-Rosas et al. 2004).
47. Articular face shape on anterior caudal centra: non-procoelous (0); slightly procoelous (1); strongly procoelous with prominent condyles (2) (modified from Salgado et al. 1997 by González Riga 2003).
48. Articular face shape on middle caudal centra: non-procoelous (0); slightly procoelous with reduced condyles (1); strongly procoelous with prominent condyles (2)

(modified from Salgado et al. 1997 by González Riga 2003).

49. Neural arch in anterior caudal vertebrae: placed in the middle of the centrum (0); anteriorly (1); on the anterior border (2) (Salgado et al. 1997).
50. Anterodorsal border of neural spine in middle caudal vertebrae located posteriorly with respect to anterior border of the postzygapophyses: absent (0); present (1) (Salgado et al. 1997).
51. Anteriorly directed anterior caudal neural spine: absent (0); present (1) (Calvo et al. 2007).
52. Shape of the section of neural spines in most anterior caudal vertebrae in dorsal view: axially elongated (0); transversely elongated (1); quadrangular (2) (Calvo et al. 2007).
53. Neural spine in middle caudal vertebrae, shape: short anteroposteriorly (0); laminated and anteroposteriorly elongated (1) (modified from González Riga 2003 by Bonaparte et al. 2006).
54. Length proportions of prezygapophyses with respect to the centrum length in middle caudal vertebrae: shorter than 50% (0); between 40% and 50% (1); longer than 50% (2) (modified from González Riga 2003).
55. Ventral depression divided by a longitudinal septum in anterior and middle caudal vertebrae: absent (0); present (1) (Salgado and Azpilicueta 2000).
56. Postzygapophyseal process in middle caudal vertebra: absent (0); present (1) (Calvo et al. 2007).
57. Well-developed interprezygapophyseal lamina in middle caudal vertebrae: absent (0); present (1) (Calvo et al. 2007).
58. Scapular glenoid orientation: relatively flat (0); strongly bevelled medially (1) (Wilson and Sereno 1998).
59. Humerus, breadth of proximal end with respect to the total length: less (0); or more (1) than the 50% (González Riga 2003).
60. Humerus, type of proximal border: strongly curved (0); straight or slightly curved (1); sigmoidal (2) (modified from Upchurch 1998 by González Riga 2002).
61. Ulnar olecranon process, development: prominent, projecting above proximal articulation (0); rudimentary, level with proximal articulation (1) (Wilson and Sereno 1998).
62. Sternal plates, shape: suboval (0); semilunar (1) (Salgado et al. 1997).
63. Semilular sternal plate with straight posterior border: absent (0); present (1) (González Riga 2003).
64. Coracoid, shape: suboval (0); quadrangular (1) (Salgado et al. 1997).
65. Metacarpals, distal phalangeal articular facets: present (0); absent (1) (Salgado et al. 1997).
66. Pubis, length with respect to ischium length: shorter or equal (0); longer (1) (Salgado et al. 1997).
67. Ischium, posterior process twice or more the length of pubis articulation: present (0); absent (1) (modified from Salgado et al. 1997 by Calvo and González Riga 2003).
68. Ischium, iliac pedicel: short and poorly developed (0); slender and well developed (1); wide and well developed (2) (Calvo and González Riga 2003).
69. Shape of preacetabular lobe of ilium: moderately expanded (0); broadly expanded and directed upward (1) (Salgado et al. 1997).
70. Orientation of preacetabular lobe of ilium: nearly vertical (0); nearly horizontal and laterally projected (1) (Salgado et al. 1997).
71. Relative orientation of the pubic peduncle of ilium: angled (0); perpendicular with respect to the sacral axis (1) (Salgado et al. 1997).
72. Humerus femoral ratio of 0.90 or more: absent (0); present (1) (McIntosh 1990).
73. Lateral bulge of femur, below the greatertrochanter: absent (0); present (1) (McIntosh 1990).
74. Femoral distal condyles, articular surface shape: restricted to distal portion of femur (0); expanded onto anterior portion of femoral shaft (1) (Wilson 2002).
75. Distal end of tibia broader transversely than anteroposteriorly: absent (0); present (1) (Salgado et al. 1997).
76. Tibial robustness: gracile, RI $\leq$ 0.3 (0); robust, RI $>$ 0.3 (1).
77. Metatarsal I, length: shortest metatarsal (0); metatarsal V shorter tan metatarsal I (1) (Curry Rogers 2005).